Sulfur dynamics during long-term ecosystem development

Benjamin L. Turner, Leo M. Condron, Christine A. M. France, Johannes Lehmann, Dawit Solomon, Duane A. Peltzer & Sarah J. Richardson

Biogeochemistry
An International Journal

ISSN 0168-2563

Biogeochemistry
DOI 10.1007/s10533-016-0208-6

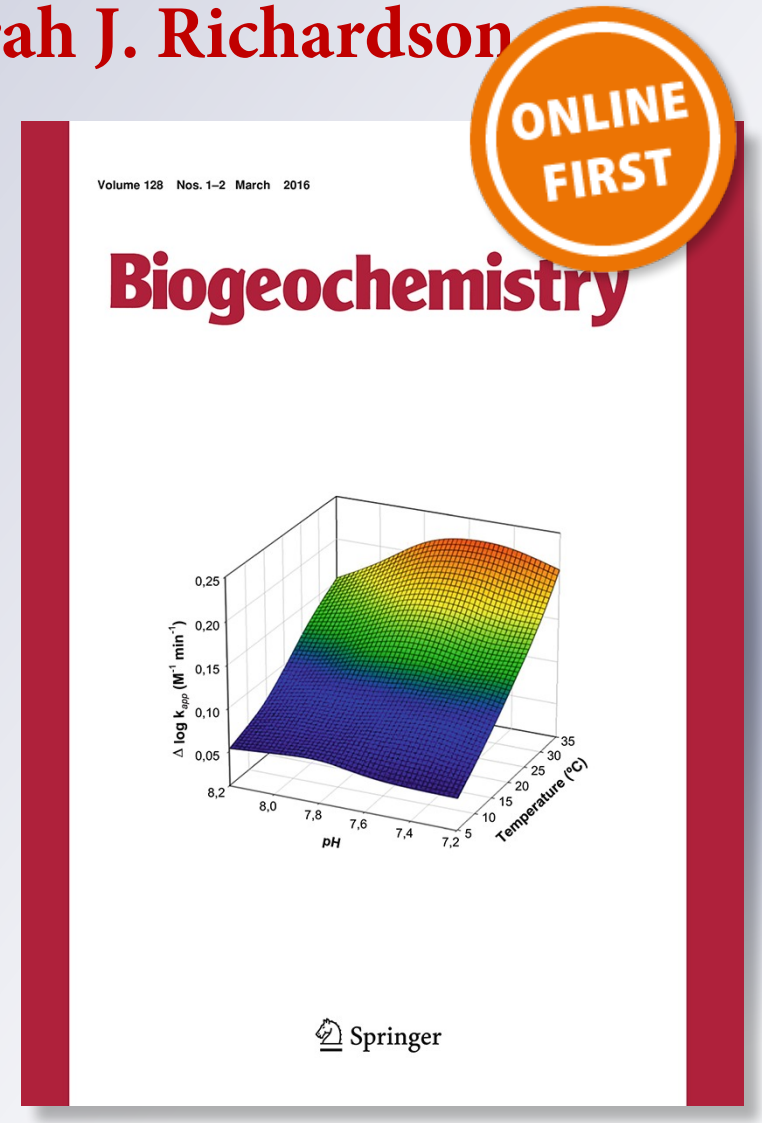

Springer

Biogeochemistry
DOI 10.1007/s10533-016-0208-6

Sulfur dynamics during long-term ecosystem development

Benjamin L. Turner · Leo M. Condron · Christine A. M. France · Johannes Lehmann · Dawit Solomon · Duane A. Peltzer · Sarah J. Richardson

Received: 21 May 2015 / Accepted: 5 April 2016

Abstract Long-term soil and ecosystem development involves predictable changes in nitrogen (N) and phosphorus (P) availability and limitation, but far less is known about comparable changes in sulfur (S) despite its importance as an essential plant macronutrient and component of soil organic matter. We used a combination of elemental analysis, X-ray absorption spectroscopy, hydrolytic enzyme assays, and stable S isotope ratios to examine S in soil and leaf tissue along the 120,000-year Franz Josef chronosequence, New Zealand. Total soil S concentrations increased during the early stages of pedogenesis and then declined as soils aged. There was little variation in soil N:S ratios along the chronosequence other than in the youngest (5 year old) soil, although the carbon (C):S ratio increased markedly in the oldest soils and the P:S ratio decreased continuously along the chronosequence. Foliar S concentrations and N:S ratios varied widely among common plant species but did not change consistently with increasing soil age, although foliar P:S declined for several species in the older stages of the chronosequence. The chemical nature of soil organic S extracted from mineral and organic horizons and determined by S *K*-edge X-ray absorption near-edge fine-structure (XANES) spectroscopy was dominated by C-bonded S distributed approximately equally in highly-reduced and intermediate oxidation states, although ester-bonded S was also abundant throughout the chronosequence. Soil sulfatase activity expressed on a soil C basis was highest in young soils, indicating low S availability in the early stage of pedogenesis. Enzymatic C:S and N:S ratios varied little during ecosystem development, although the enzymatic P:S ratio increased continuously along the chronosequence. Stable S isotope ratios ($\delta^{34}S$)

Responsible Editor: Steven Perakis.

Electronic supplementary material The online version of this article (doi:10.1007/s10533-016-0208-6) contains supplementary material, which is available to authorized users.

B. L. Turner (✉)
Smithsonian Tropical Research Institute, Apartado 0843-03092, Balboa, Ancon, Republic of Panama
e-mail: TurnerBL@si.edu

L. M. Condron
Agriculture and Life Sciences, Lincoln University, P.O. Box 84, Lincoln 7647, New Zealand

C. A. M. France
Museum Conservation Institute, Smithsonian Institution, 4210 Silver Hill Road, Suitland, MD 20746, USA

J. Lehmann · D. Solomon
Department of Soil and Crop Sciences, Atkinson Center for a Sustainable Future, Cornell University, Ithaca, NY 14853, USA

D. A. Peltzer · S. J. Richardson
Landcare Research, P.O. Box 69040, Canterbury, Lincoln 7640, New Zealand

Published online: 21 April 2016

increased along the chronosequence, particularly in the early stages of pedogenesis, reflecting a shift in S inputs from primary mineral S to oceanic sulfate in atmospheric deposition. Overall, this first comprehensive assessment of S along a long-term soil chronosequence suggests that S availability is low in the earliest stage of pedogenesis, but then remains stable throughout the progressive and retrogressive phases of ecosystem development, despite pronounced shifts in the chemistry and dynamics of other nutrients.

Keywords Sulfatase · Pedogenesis · Stable isotopes · $\delta^{34}S$ · XANES spectroscopy · Franz Josef chronosequence · Stoichiometry

Introduction

Nutrient transformations during long-term ecosystem development influence the productivity, composition, and diversity of plant and microbial communities (Vitousek 2004; Wardle et al. 2004; Turner and Condron 2013; Laliberté et al. 2014). In particular, nitrogen (N) and phosphorus (P) follow predictable patterns as pedogenesis proceeds. Nitrogen availability is low at the onset of soil formation, but increases rapidly through biological N fixation (Vitousek et al. 1989). In contrast, P is relatively abundant in young soils, but declines continuously during pedogenesis as it is lost in runoff at a greater rate than it is supplied from bedrock weathering or atmospheric deposition (Walker and Syers 1976). This leads to a theoretical prediction that N limits primary productivity on young soils, whereas P limits productivity on old soils, which has now been verified on contrasting long-term chronosequences (Vitousek and Farrington 1997; Laliberté et al. 2012; Coomes et al. 2013). In some cases, P limitation becomes so severe on old, stable surfaces that it leads to a decline in biomass and productivity, termed ecosystem retrogression (Wardle et al. 2004; Peltzer et al. 2010).

Sulfur (S) is an essential macronutrient that forms a quantitatively important component of plant tissue and soil organic matter (Freney and Williams 1983; Marschner 2006). Yet in contrast to N and P, the dynamics of S have been largely overlooked in studies of ecosystem development. In a review of S dynamics in forest ecosystems, Mitchell et al. (1992) highlighted the evaluation of changes in organic S constituents in ecosystems over extended periods of time as a key research priority. However, the dynamics of S during long-term ecosystem development remain poorly understood, because only a handful of studies have measured S along soil chronosequences (Syers et al. 1970; Jehne and Thompson 1981; Prietzel et al. 2013; Bern et al. 2015). For example, Syers et al. (1970) found that the soil S stock initially declined in the first 50 years of pedogenesis along a coastal dune chronosequence in New Zealand, but then accumulated in parallel with organic carbon (C) during the following 10,000 years. However, the rate of increase in soil S (0.15 kg S ha^{-1} $year^{-1}$) was much less than the rate of atmospheric S deposition (10 kg ha^{-1}). Prietzel et al. (2013) examined soil S chemistry along two young glacial foreland chronosequences, finding a rapid decline in primary mineral S and accumulation of S in organic forms in the first few decades of pedogenesis. This agrees with modeling studies (e.g., Parton et al. 1988) and indicates that recycling of S from organic matter quickly becomes an important source of S for biological uptake, at least where atmospheric S deposition is low (Mitchell et al. 1992). Recently, Bern et al. (2015) examined stable S isotope ratios along the 4.1 million year Hawaiian Island chronosequence, finding an increase in ^{34}S with site age in both soils and vegetation that reflected a decreasing contribution of volcanic aerosols compared to marine sulfate to the ecosystem S budget.

Sulfur deficiency occurs commonly in regions that do not receive pollutant S deposition from the atmosphere, including southeastern Australia, New Zealand, and the Northwest USA (Johnson 1984). In addition, agricultural S deficiency is becoming widespread in Europe and elsewhere, as atmospheric S deposition declines and farmers switch to fertilizers that contain relatively low amounts of S (McGrath and Zhao 1995; Mathot et al. 2008). Although most evidence points to a shift from N and P limitation as pedogenesis proceeds, it is conceivable that productivity might be temporarily limited by S availability during the period commonly assumed to be co-limited by N and P (i.e. when N accumulation has peaked, but P is still in relatively plentiful supply) (Vitousek and Farrington 1997; Laliberté et al. 2012). Alternatively, forest productivity might be limited by multiple elements simultaneously, including N, P, S, and other

nutrients (e.g. Wright et al. 2011). These scenarios are most likely to occur in regions remote from sources of marine or anthropogenic S deposition.

Sulfur deficiency does not necessarily manifest as a direct reduction in forest productivity, but can influence plant performance and species distributions through resistance to pathogens or by affecting the availability and acquisition of other nutrients. For example, S deficiency can constrain biological N fixation by legumes by suppressing nitrogenase activity (Walker and Adams 1958; Marschner 2006), which might in turn influence productivity in the N-limited progressive stage of ecosystem development. Indeed, biological N fixation is perhaps more likely to be constrained by S than by P on young soils, given that primary mineral S appears to be depleted relatively rapidly compared to primary mineral P under humid temperate climates (Parton et al. 1988; Prietzel et al. 2007). Sulfur availability might also be influenced by P availability, because S uptake by plants can be inefficient under conditions of P deficiency, even if sulfate is abundant in solution (Smith et al. 1985). Sulfur uptake by plants might therefore be constrained by P limitation in the retrogressive stage of ecosystem development.

Sulfur occurs in plant tissue primarily as amino acids, principally cysteine and methionine (Marschner 2006). In contrast, soil organic S occurs in a variety of chemical forms of varying oxidation and bonding states, including C-bonded S (e.g. amino acids) and ester-bonded S (i.e. C–O–S bonds) (Stevenson and Cole 1999). Like P, microbes can obtain S from organic compounds via either biological or biochemical mineralization (McGill and Cole 1981). Biological mineralization involves the oxidation of C–S bonds and occurs as microbes metabolize organic matter to provide energy. In contrast, biochemical mineralization involves the hydrolysis of ester bonds and is catalyzed by sulfatase enzymes released by microbes in response to a demand for S. The amount of C-bonded S in soil organic matter is therefore expected to vary in response to processes driving C oxidation in soil organic matter, whereas ester-bonded S is expected to vary in response to changes in the biological demand for S. Although some results support this hypothesis for S (e.g., Maynard et al. 1984), it has not been widely tested. Indeed, it has been suggested that C-bonded S might be more dynamic than ester-bonded S, based on a decline in reduced S forms during land-use change (Solomon et al. 2003; Zhao et al. 2006).

During ecosystem development, S availability and limitation, or an influence of N or P limitation on S acquisition, might be detected in several ways, including changes in leaf tissue chemistry and soil organic matter. These changes might include:

(i) Soil S concentrations and nutrient stoichiometry (i.e., C:S, N:S, or P:S ratios), with greater ratios reflecting a greater biological demand for S relative to other nutrients.

(ii) Foliar S concentrations and nutrient stoichiometry, with lower foliar S and greater C:S or N:S ratios indicating reduced S availability (Lambert and Turner 1998).

(iii) The chemical nature of soil organic S, with increasing S demand reflected in the depletion of ester-bonded S (i.e. reflecting biochemical mineralization) compared to C-bonded S (reflecting biological mineralization) (McGill and Cole 1981).

(iv) Soil sulfatase activity and enzyme stoichiometry (i.e. the ratios of enzymes involved in the acquisition of C, N, or P to sulfatase activity), with greater sulfatase activity and narrower enzymatic C:S, N:S, or P:S ratios indicating greater S demand by the microbial community (Sinsabaugh et al. 2009).

(v) Stable S isotopes (i.e. the ^{34}S:^{32}S ratio, expressed as $\delta^{34}S$) in soils, with lower ratios (i.e. more depleted values) indicating a tighter S cycle with less fractionating losses and greater S demand. This is analogous to the use of $\delta^{15}N$ as an integrative measure of the terrestrial N cycle, with greater N availability leading to a more open N cycle and greater gaseous loss of depleted N by denitrification (e.g., Hobbie and Ouimette 2009; Hietz et al. 2011). For example, a more open S cycle might be reflected in relatively enriched soil $\delta^{34}S$ due to high leaching losses of ^{34}S-depleted sulfate (Mayer et al. 1995). However, a number of other factors can influence soil $\delta^{34}S$ (Bern et al. 2015) and there is relatively little information on which to base interpretation of soil $\delta^{34}S$ values.

To evaluate S dynamics and indicators of potential S availability and limitation during long-term

ecosystem development, we used a combination of elemental analysis, X-ray absorption spectroscopy, hydrolytic enzyme assays, and stable S isotope ratios to examine soils and leaf tissue along a 120,000 year postglacial chronosequence at Franz Josef, on the west coast of the South Island of New Zealand. The Franz Josef chronosequence provides an ideal framework to examine long-term changes in S dynamics because (i) it is well characterized, with a detailed understanding of changes in relative N and P availability and limitation and plant community composition during ecosystem development, and (ii) it has received minimal anthropogenic S deposition from the atmosphere due to its location on the west coast of the South Island of New Zealand (Vet et al. 2014). The Franz Josef chronosequence therefore offers the opportunity to study S dynamics during long-term ecosystem development along a natural pedogenic gradient without the confounding effects of anthropogenic S deposition.

Methods

The Franz Josef chronosequence

The Franz Josef post-glacial chronosequence is well studied (Walker and Syers 1976; Parfitt et al. 2005; Wardle et al. 2004; Richardson et al. 2004; Turner et al. 2007; Holdaway et al. 2011) and patterns of C, N, and P transformations are representative of chronosequences more broadly (Peltzer et al. 2010). Briefly, the chronosequence consists of a series of post-glacial surfaces up to 120,000 years old on the west coast of the South Island of New Zealand (Table 1; Fig. 1). All sites are <270 m a.s.l. Mean annual temperature is 10.8 °C and annual rainfall varies from ~7500 mm at young sites in the glacial valley to ~4000 mm at older sites nearer the coast (Table 1). These rainfall estimates update those reported previously by Richardson et al. (2004), because improvements to the underlying digital elevation model now capture the intense rainfall gradients in the region. The soils support mixed conifer–angiosperm forests, with young sites dominated by evergreen angiosperms and older sites supporting an increasing proportion of conifers in the Podocarpaceae (Wardle 1980; Richardson et al. 2004). All sites are composed of schist deposits, although infertile quartz silt loess was deposited on the two oldest sites during the last glaciation (Almond et al. 2001). Despite this, the sequence represents a clear age-related nutrient gradient that influences both above and below ground biological communities (Allison et al. 2007; Holdaway et al. 2011; Richardson et al. 2004; Jangid et al. 2013; Turner et al. 2013; Wardle et al. 2004; Williamson et al. 2005).

Atmospheric sulfur inputs

Anthropogenic S deposition in the region is estimated from a global-scale model to be <1 kg S ha^{-1} per year (Vet et al. 2014). However, the chronosequence probably receives significant atmospheric S deposition from oceanic sources. For example, rates of atmospheric S deposition at Haast and Whataroa, both on the west coast of the South Island of New Zealand, were reported to be approximately 10 kg S ha^{-1} per year (Ledgard and Upsdell 1991). We estimated atmospheric S deposition for each of the ten chronosequence sites using a model derived from S deposition data from locations on the west coast of the South Island of New Zealand (Eq. 7 in Ledgard and Upsdell 1991). The model describes a logarithmic decline in S deposition with distance from the coast, which can be estimated using information on mean annual precipitation and distance to the coastline: $\log_e(\text{kg S ha}^{-1}\text{ year}^{-1}) = 2.53 - 0.021 \times (\text{distance to coastline, km}) - 6.6 \times 10^{-5} \times (\text{annual rainfall, mm})$.

Soil and plant tissue sampling and preparation

Five replicate samples were taken from the organic horizon and upper 10 cm of mineral soil at each of ten sites along the chronosequence over three days in the southern hemisphere winter of 2005. The sites ranged in age from 5 years to 120,000 years and have been described in detail previously (Stevens 1968; Almond et al. 2001; Richardson et al. 2004; Allison et al. 2007). No organic horizon was present at the 5 year old site. Soils were sieved (<4 mm) and small stones and fine roots were removed manually. Subsamples of each soil were stored at 4 °C prior to enzyme assays. The remaining samples were air-dried and ground prior to analysis.

Leaf tissue was collected from a number of species along the chronosequence (Richardson et al. 2005), of which eight species with distributions spanning a

Table 1 Description of studied stages along the Franz Josef post-glacial chronosequence, including estimated atmospheric sulfur deposition

Site	Age[a] (year)	Landform	Elevation (m asl)	Precipitation[b] (mm year^{-1})	Distance to coast (km)	Sulfur deposition[c] (kg S ha^{-1} year^{-1})
1	5	Terrace slip	230	7449	16.4	5.4
2	60	River terrace	239	7514	16.5	5.4
3	130	River terrace	220	6943	16.1	5.7
4	280	River terrace	199	6943	16.4	5.6
5	530	Outwash surface	201	6956	16.2	5.7
6	1000	River terrace	211	6479	15.2	6.0
7	5000	Kame terrace	232	7017	15.2	5.7
8	12,000	Kame terrace	263	4128	12.4	7.4
9	60,000	Moraine	252	4032	10.3	7.7
10	120,000	Moraine	142	4076	4.5	8.7

[a] The sites were described by Stevens (1968), with the dates of older sites updated by Almond et al. (2001)

[b] Estimated for each site using elevation and geographic location from thin-plate splines fitted to data from nearby meteorological stations. These values update those reported previously (Richardson et al. 2004), because improvements to the underlying digital elevation model now capture the intense rainfall gradients in the region

[c] Calculated from equation [7] in Ledgard and Upsdell (1991), derived from elevation and distance to the nearest coastline for locations on the west coast of New Zealand: $\log_e$(kg S ha^{-1} year^{-1}) = 2.53 − 0.021 × (distance to coastline, km) − 6.6 × 10^{-5} × (annual rainfall, mm)

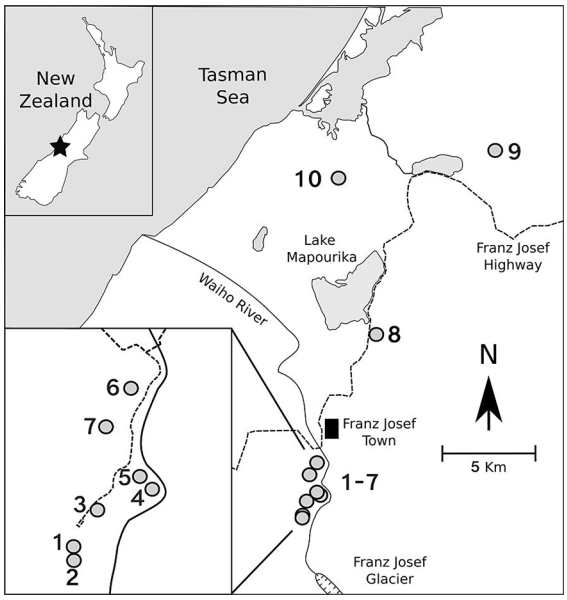

Fig. 1 Map of sampling sites along the Franz Josef post-glacial chronosequence, New Zealand. Sites increase in age from site 1 (5 years) to site 10 (120,000 years) and are described in Table 1

considerable proportion of the chronosequence are included here. Species represented ≥5 % of the total canopy cover at a given site, except for some widespread species and species at the youngest site where no species accounted for ≥5 % of the canopy (we selected two common species to represent the youngest site). Leaves were dried at 60 °C and ground prior to analysis.

Elemental analysis of soils and plant tissue

Total C, N, and S in soils were determined simultaneously by combustion in a Leco CNS-2000 analyzer (LECO Corporation, St Joseph, MI, USA), hereafter referred to as elemental analyzer (EA). Initially, total C and N were determined on each individual replicate at each sequence stage. Subsequently, C, N, and S were determined on composite samples of the five replicate plots at each site. Total soil S was also determined on individual replicates using a Costech EA with detection by isotope ratio mass spectrometry, hereafter referred to as IRMS (see below). Organic P was determined as the difference in P extracted in 1 M H_2SO_4 in samples that had been ignited at 550 °C for 1 h and unignited samples (Walker and Adams 1958). Phosphorus in ignited samples was assumed to represent total soil P. Phosphorus analysis was conducted on composite samples of the five replicate plots at each site. All elemental ratios in soils were calculated for composite samples analyzed by EA. We did not quantify readily soluble sulfate along the

sequence, because although this could provide an indication of potentially plant available sulfate, such measurements are widely regarded as providing a poor indication of S availability to plants (Reimann et al. 2003; Haneklaus et al. 2007). Foliar N and P analysis and concentrations were reported previously (Richardson et al. 2005). Foliar S was determined by IRMS (see below). All elemental ratios are expressed on a mass basis. Differences in foliar nutrient concentrations among sites were tested across sites (using the mean value for a species at a site) and within species (using all replicate values of a species at a site). We used ANOVA for factors with ordered levels (function *ordAOV* in the R library *ordPens*) to test for directional shifts in foliar nutrients along the sequence. Sites are ordered from 1 to 9 in this analysis but no assumptions are made about the distance between those sites (either in terms of their age or nutrient status) (Gertheiss 2014).

Sulfur K-edge XANES spectroscopy

Investigation into the chemical nature of soil organic S has conventionally been restricted to the estimation of broad operationally defined groups by wet chemistry procedures (Tabatabai 1996). However, the development of S *K*-edge X-ray absorption near-edge fine-structure (XANES) spectroscopy for soil S analysis has yielded important insight into soil organic S chemistry (e.g. Solomon et al. 2003), including changes during pedogenesis (Prietzel et al. 2013; Tanikawa et al. 2014). The technique has considerable advantages over conventional wet chemical procedures for the speciation of soil organic S, because it provides detailed information on chemical composition without the need for sequential extraction schemes that provide little structural insight (e.g., Morra et al. 1997).

Organic S was analyzed by X-ray absorption spectroscopy following separation of organic S from the remainder of the soil matrix (including inorganic S) as described previously (Solomon et al. 2003; Lehmann et al. 2008). Organic S was extracted in a solution containing 0.1 M NaOH and 0.4 M NaF in a 1:5 (w/v) soil-to-solution ratio under N_2. This alkali-extractable organic S approximates the total organic S (e.g., Fig. 2 in Solomon et al. 2003) and we assume that this in turn represents total S in the majority of the soils studied here, given that inorganic S disappears rapidly in the very early stages of pedogenesis (Prietzel et al. 2013). Analyses of unextracted samples gave similar spectra to those reported previously in such comparisons (Solomon et al. 2003), but these were more difficult to interpret due to fused peaks and high signal to noise in the reduced S region of the spectra. For each chronosequence stage, samples of mineral soil and the organic horizon from the five replicate plots were extracted separately and then combined to yield a single composite sample for the mineral horizon and one for the organic horizon per chronosequence stage. Extracts were dialyzed (Spectra/Por Membrane, MWCO, 12,000–14,000 Da; Spectrum Laboratories, CA) and freeze-dried.

Sulfur *K*-edge XANES spectroscopy was conducted at beamline X-19A of the National Synchrotron Light Source (NSLS), at Brookhaven National Laboratory, USA. Scans ranging from 150 eV below to 300 eV above the absorption edge of S at 2472 eV (calibrated with elemental S) were collected with a step size of 0.2 eV. Each XANES spectrum was composed of an average of three scans. A monochrome consisting of a double crystal Si (111) with an entrance slit of 0.5 mm and a minimum energy resolution of 2×10^{-4} (0.5 eV) at the S *K*-edge was used. The spectra were recorded in fluorescence mode using a passivated implanted planar silicon (PIPS) detector (Canberra Industries, CT).The beampath from the incident ion chamber to the sample chamber was purged with helium. The samples were pressed into a 0.5 mm deep acrylic holder and covered with 2.5 μm thick Mylar film (Complex Industries, NY).

Deconvolution of XANES spectra for each sample into pseudo-components was performed using the nonlinear least squares fitting routine solver of Microsoft Excel (Xia et al. 1998). The XANES spectra were fitted using a series of Gaussian curves (G1, G2, G3, G4, and G5) that represent the sfp transitions (white line) and arctangent step functions (AT1 and AT2) of the transitions of ejected photoelectrons to the continuum (step height or background). These Gaussian curves correspond to oxidation states and organic S forms (Solomon et al. 2003). Specifically, the G1 group consists of thiols (R–S–H) and sulfides (R–S–R′, R–S–S–R′, etc.) with oxidation states between 0.14 and 0.38 eV. The G2 group includes thiophenes (aromatic heterocyclic compounds) with oxidation states between 0.80 and 0.96. The G3 group contains sulfoxides (R–SO–R′) with oxidation states between

1.25 and 1.82. The G4 group contains sulfonates (R–SO_3–H) with an oxidation state of 5.00. The G5 group represents ester sulfates (R–OSO_3–H) with an oxidation state of 6.00. We further group these into highly reduced S (G1 + G2), S in intermediate oxidation states (G3 + G4), and total C-bonded S (G1 + G2 + G3 + G4). We also calculated the following ratios as indicators of change in the chemical nature of soil organic S:

(i) C-bonded S: ester-bonded S (G1 + G2 + G3 + G4 / G5)
(ii) Oxidized S: reduced S (G3 + G4 + G5: G1 + G2) (Lehmann et al. 2008; Prietzel et al. 2013)
(iii) S in intermediate oxidation states: highly oxidized S (G3 + G4: G5) (Solomon et al. 2009)

Finally, Schroth et al. (2007) demonstrated variation in the behavior of soil organic S groups during litter decomposition in mineral soil, involving a decrease in the proportion of sulfides and sulfoxides and an increase in the proportion of sulfonates and ester sulfates. We therefore also calculated a 'decomposition index' using the ratio of sulfides and sulfoxides (G1 + G2 + G3) to sulfonates and sulfates (G4 + G5).

Hydrolytic enzyme assays

Sulfatase data were reported previously on the basis of dry soil and phospholipid fatty acids (Allison et al. 2007). Here we recalculated these values on the basis of soil C, to infer comparable patterns of S demand in mineral soil and organic horizons along the chronosequence. Sulfatase activity was assayed on fresh soil using 4-methylumbelliferyl-sulfate as a substrate analogue (Allison et al. 2007). Assays were conducted in micro-well plates using 50 mM sodium acetate buffer at pH 5.0 and incubated at 20 °C, with corrections for quenching and auto-fluorescence of both sample and substrate. Sulfatase activity was expressed on the basis of soil organic C to standardize across soils with marked differences in organic matter. Ratios of activities of enzymes involved in the cycles of C (β-glucosidase), N (*N*-acetyl-glucosaminidase), and P (acid phosphomonoesterase) to sulfatase were calculated using data from Allison et al. (2007). Sulfatase activity was not determined for the youngest site (5 years old).

Sulfur stable isotope ratios

Sulfur stable isotope ratios (^{34}S:^{32}S, expressed as $\delta^{34}S$) were determined in organic and mineral soils using an elemental analyzer (Costech, Valencia, CA, USA) coupled to a Delta V Advantage isotope ratio mass spectrometer through a Conflo-IV interface (Thermo, Bremen, Germany). Vanadium pentoxide was added to each sample to improve combustion. Values were calibrated using a three-point linear correction to sulfide and sulfate standards (IAEA-S1, IAEA-S2, IAEA-SO6) and are expressed in per mil (‰) relative to the international Vienna Canyon Diablo Troilite standard (Krouse and Coplen 1997) using the equation:

$$\delta^{34}S = \left(R_{sample}/R_{standard} - 1\right) \times 1000$$

where $R = {}^{34}S/{}^{32}S$. All values incorporate an error of ±0.2 ‰.

Results

Estimated atmospheric sulfur deposition

The majority of sites along the chronosequence (between 5 and 5000 years) were located in the glacial valley (Fig. 1) at similar elevation (199–239 m asl), annual precipitation (6479–7514 mm) and distance to the coastline (15.2–16.5 km) (Table 1). As a consequence, estimated atmospheric S deposition at these sites varied little, ranging between 5.4 and 6.0 kg S ha^{-1} $year^{-1}$ (Table 1). In contrast, the older sites along the chronosequence were on the coastal plain, closer to the coastline (12.4 km at the 12,000 year site to 4.5 km at the oldest site) with less annual precipitation (4032–4128 mm). Estimated atmospheric S deposition at these older sites was therefore greater than in the upper valley, ranging between 7.4 and 8.7 kg S ha^{-1} $year^{-1}$ (Table 1). Further, based on Fig. 2 in Ledgard and Upsdell (1991) we estimate that the contribution of sea spray to the total atmospheric S input varies from 60 to 65 % for the oldest three sites to about 50–55 % for the remainder of the sites, although the relationship

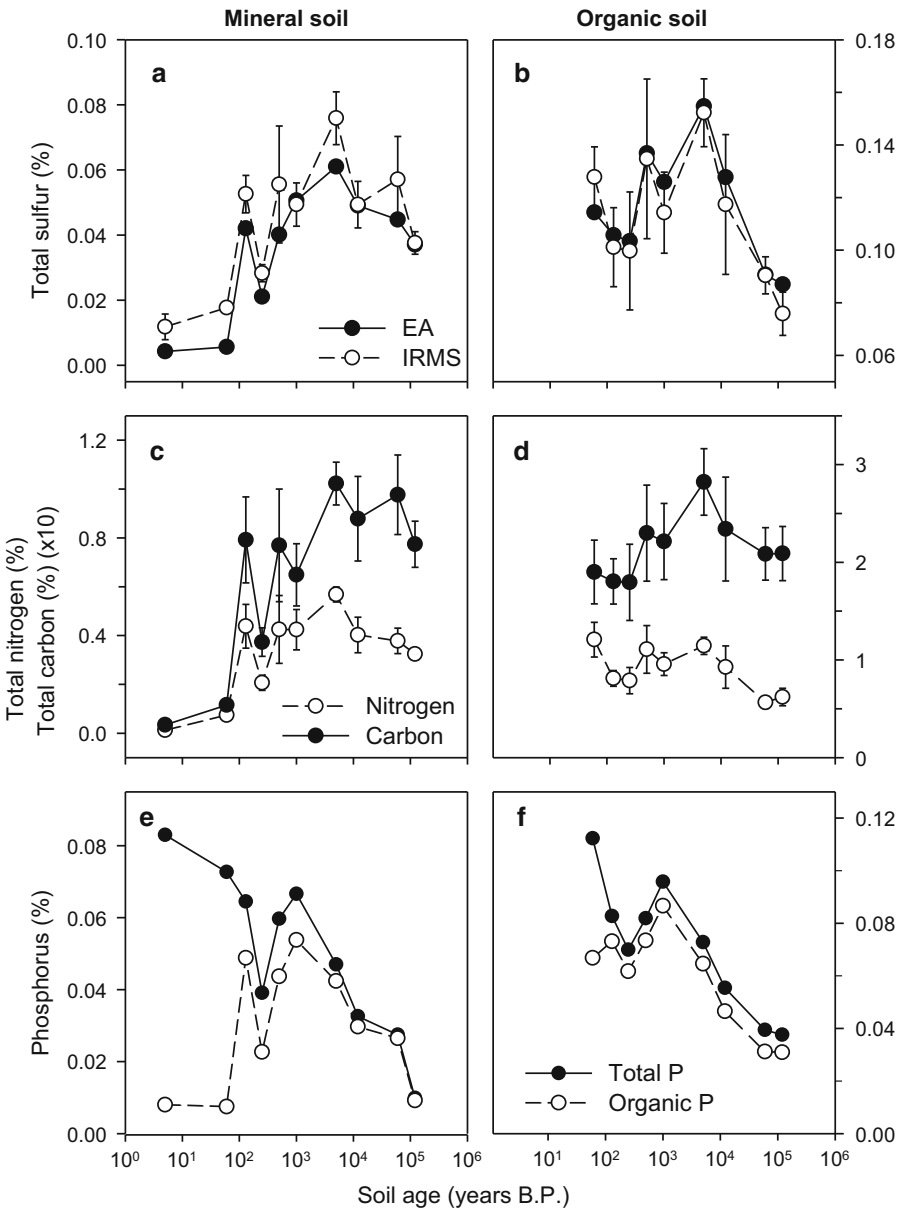

Fig. 2 Total element concentrations in mineral soil (*left panel*) and the organic horizon (*right panel*) along the 120,000 year Franz Josef post-glacial chronosequence, New Zealand. Sulfur concentrations (plots **a**, **b**) include values determined by elemental analyzer (EA, *filled symbols* and *solid line*) and isotope ratio mass spectrometry (IRMS, *open symbols* and *dashed line*). Values determined by IRMS are mean ± standard error of five replicate plots at each site, while values determined by EA are of composite samples from five replicate plots at each site. Total soil carbon (C, *closed symbols* and *solid line*) and nitrogen (N, *open symbols* and *dashed line*) (plots **c**, **d**) were the means of five replicate plots per site and the total C values are × 10 compared to the *Y* axis. For phosphorus (P) (plots **e**, **f**), values for total P (*filled symbols* and *solid line*) and organic P (*open symbols* and *dashed line* were determined on a single composite sample from each site. All error bars are standard errors

presented in Ledgard and Upsdell (1991) was based only on distance to the coastline and shows considerable variation close to the coast.

Total S concentrations in soils

Total S concentrations in mineral soil increased from low levels in very young soils (<0.001 %) to a maximum of 0.061 % after 5000 years of soil development, and then declined to ~0.04 % in the oldest soils (120,000 years) (Fig. 2a). A marked increase in total S, as well as in C, N, and P, occurred in the 130 year old soil. Total S concentrations in the organic horizon were relatively low in young soils (~0.10 %), increased to a maximum of 0.15 % after 5000 years, and then declined to the lowest concentrations in the oldest soils (~0.09 %) (Fig. 2b).

The changes in soil S during pedogenesis corresponded closely to patterns of soil C and N concentrations, which increased initially in young mineral soils to maximum values at around 5000 years (Fig. 2c). Total C concentrations were then relatively

constant throughout the remainder of the chronosequence, whereas N concentrations declined in older soils. In the organic horizon, C concentrations were much greater than in mineral soils, but followed a similar pattern, increasing in the early stages and then declining in old soils (Fig. 2d). Nitrogen initially declined from 60 to 130 years, and then followed a similar pattern to total C, increasing and then declining in older soils. Organic P concentrations also followed a similar pattern to total S, increasing initially in the early stages of pedogenesis, and then declining in old soils, for both mineral and organic horizons (Fig. 2e, f). In contrast, total P concentrations (i.e. organic plus inorganic P) declined more or less continually throughout the chronosequence in both mineral and organic horizons (Fig. 2e, f). Overall, total soil S was strongly correlated with total soil C, total soil N, and to a lesser extent soil organic P (Fig. 3).

Total element ratios in soils

The C:S ratio (mass basis) increased continuously throughout the chronosequence in both mineral and organic horizons (Fig. 4a). In mineral soil, the C:S ratio increased from 76 in the youngest soil to approximately 180 for much of the sequence, before increasing again to >220 in the two oldest soils. Similarly in the organic horizon, the C:S ratio was about 170 in the early part of the chronosequence, and then increased to >250 in the oldest soils (Fig. 4a). In the early stages of the chronosequence the C:S ratios were similar in mineral and organic horizons, but gradually increased in the organic horizon of older soils. Mean C:S ratios across the chronosequence (excluding the youngest mineral soil) were 181 ± 31 in mineral soil and 198 ± 37 in the organic horizon (mean ± standard deviation of nine sites).

The N:S ratio was very low (1.11) in the youngest (5 year old) mineral soil, indicating the presence of inorganic S in primary minerals in the parent material (Fig. 4b). However, the N:S ratio increased rapidly and remained stable throughout the remainder of the chronosequence (mean 9.11 ± 0.69). In the organic horizon, the N:S ratio was 10.2 in the 60 year old soil, but then declined and remained stable throughout the remainder of the chronosequence (mean 8.0 ± 0.89) (Fig. 3b). Apart from the 60 year soil, the N:S ratio was greater in the mineral soil than the organic horizon throughout the chronosequence.

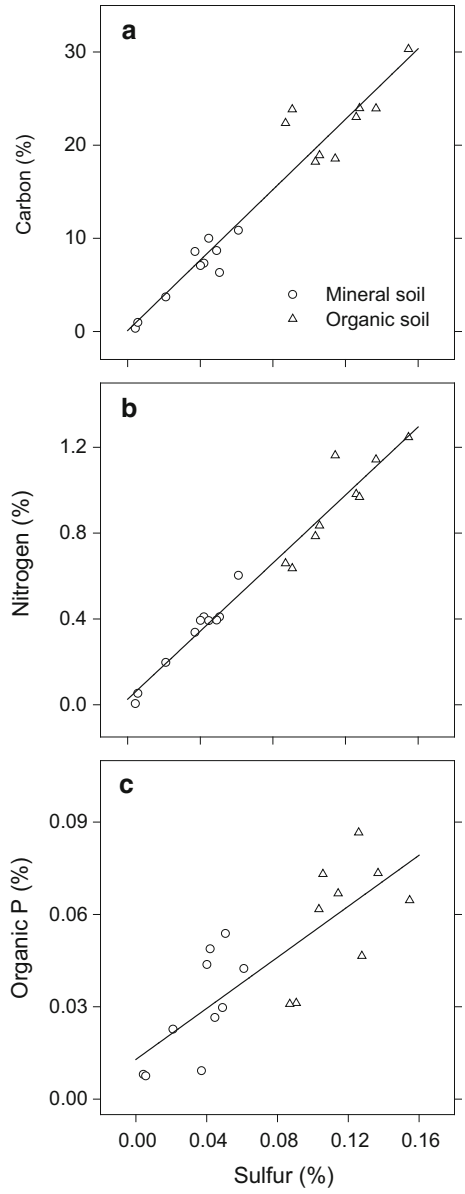

Fig. 3 Relationships between the concentrations of total soil sulfur and **a** total soil carbon, **b** total soil nitrogen, and **c** soil organic phosphorus (P), in mineral and organic horizons of soils along the 120,000 year Franz Josef post-glacial chronosequence, New Zealand. Pearson Product Moment correlation coefficients were 0.96, 0.98, and 0.81 for **a**, **b**, and **c**, respectively ($p < 0.0001$)

In contrast to the N:S ratio, the P:S ratio, expressed as either total P: total S (Fig. 4c) or organic P: total S (Fig. 4d), declined continuously throughout the chronosequence in both mineral and organic horizons. In mineral soil, the organic P:S ratio declined from

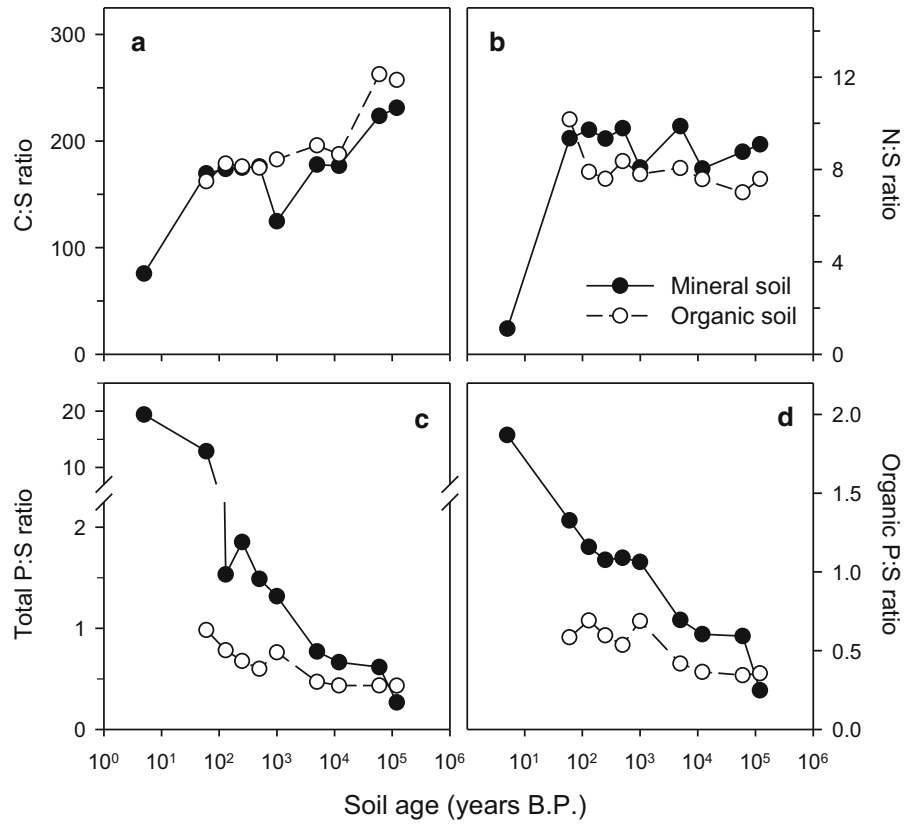

Fig. 4 Ratios of total elements in mineral soil (*filled symbols* and *solid lines*) and the organic horizon (*open symbols* and *dashed lines*) along the 120,000 year Franz Josef post-glacial chronosequence, New Zealand. The plots show **a** total carbon (C) to total sulfur (S), **b** total nitrogen (N) to total S, **c** total phosphorus (P) total S, and **d** organic P to total S. Elemental ratios were calculated using data determined on composite samples of five replicate plots at each site

1.87 in the youngest soil to 0.25 in the oldest soil (120,000 years). In the organic horizon, the ratio declined from 0.58 in the youngest soil to 0.34 in the 60,000 year old soil. The organic P:S ratio was always greater in the mineral soil (mean 0.87 ± 0.35) compared to the organic horizon (mean 0.51 ± 0.14). Total P:S was as high as 19.4 in the youngest mineral soil, declining to 1.53 after 130 years, and then 0.27 on the oldest soil. The ratios were lower in the organic horizon, declining from 0.98 in the 60 year old soil to 0.43 in the three oldest soils.

Foliar sulfur

Foliar S varied markedly among species, with species means across the chronosequence ranging between 0.08 ± 0.02 % for *Dacrydium cupressinum* to 0.39 ± 0.08 % for *Coprosma foetidissima* (Table 2). However, species showed contrasting patterns in foliar S during ecosystem development (Fig. 5; Supplementary Table 2). For example, foliar S in *D. cupressinum* and *Griselinia littoralis* increased in plants growing on older soils, whereas concentrations declined with soil age for the tree fern *Dicksonia squarrosa* (Fig. 5). In other species, such as the conifer *Prumnopitys ferruginea*, foliar S did not vary markedly along the chronosequence. Overall, the mean foliar S and N concentrations did not vary significantly along the chronosequence, although foliar P did decline significantly (Richardson et al. 2005; Supplementary Table 2).

Foliar N:S and P:S ratios

Foliar N:S ratios varied markedly among species, with species-specific mean ratios across the chronosequence ranging between 4.1 ± 0.6 for *C. foetidissima* and 13.6 ± 4.3 for *D. cupressinum* (Table 2), with an overall mean N:S ratio across species of 7.7 ± 2.8. For several species, foliar N:S declined in plants growing on the oldest soils, including *D. cupressinum*, *G. littoralis*, *Metrosideros umbellata*, *Pseudopanax crassifolius*, and *Weinmannia racemosa* (Fig. 6; Supplementary Table 1).

Table 2 Mean total element concentrations and stoichiometric ratios for dominant plant species along the 120,000 year Franz Josef post-glacial chronosequence, New Zealand

Species	Family	Total S (%)	N:S	P:S	Sites codes (number of sites)
Coprosma foetidissima	Rubiaceae	0.39 ± 0.08	4.1 ± 0.6	0.42 ± 0.16	3–9 (6)
Dacrydium cupressinum	Podocarpaceae	0.08 ± 0.02	13.6 ± 4.3	1.19 ± 0.55	7–10 (4)
Dicksonia squarrosa	Dicksoniaceae	0.22 ± 0.03	8.0 ± 0.5	0.73 ± 0.17	2–9 (7)
Griselinia littoralis	Griseliniaceae	0.13 ± 0.05	8.9 ± 3.3	1.07 ± 0.60	2–9 (7)
Metrosideros umbellata	Myrtaceae	0.16 ± 0.02	5.0 ± 1.3	0.48 ± 0.15	3–10 (7)
Prumnopitys ferruginea	Podocarpaceae	0.15 ± 0.01	6.7 ± 0.9	0.84 ± 0.26	4–9 (5)
Pseudopanax crassifolius	Araliaceae	0.12 ± 0.04	8.6 ± 1.6	0.91 ± 0.30	3–10 (7)
Weinmannia racemosa	Cunoniaceae	0.13 ± 0.04	7.3 ± 2.4	0.65 ± 0.37	2–10 (8)
All species mean		0.17 ± 0.10	7.8 ± 2.9	0.79 ± 0.27	

Values are mean ± standard deviation for each species along the sequence where the species occurs. Site ages are: 1 = 5 years, 2 = 60 years, 3 = 130 years, 4 = 280 years, 5 = 530 years, 7 = 5000 years, 8 = 12,000 years, 9 = 60,000 years, 10 = 120,000 years

S sulfur, *N* nitrogen, *P* phosphorus. Note that vegetation was not analyzed from site 6

Foliar P:S ratios also varied markedly among species, with species means across the chronosequence ranging between 0.42 ± 0.16 for *C. foetidissima* and 1.19 ± 0.55 for *D. cupressinum* (Table 2), with an overall mean N:S ratio across species of 0.80 ± 0.27. There were clear and continual declines in foliar P:S for all species as soils aged, although foliar P:S increased initially in four species (*D. squarrosa*, *G. littoralis*, *M. umbellata*, and *W. racemosa*) during the very earliest stages of ecosystem development (Fig. 7; Supplementary Table 1). The across-species mean foliar N:S ratio did not vary

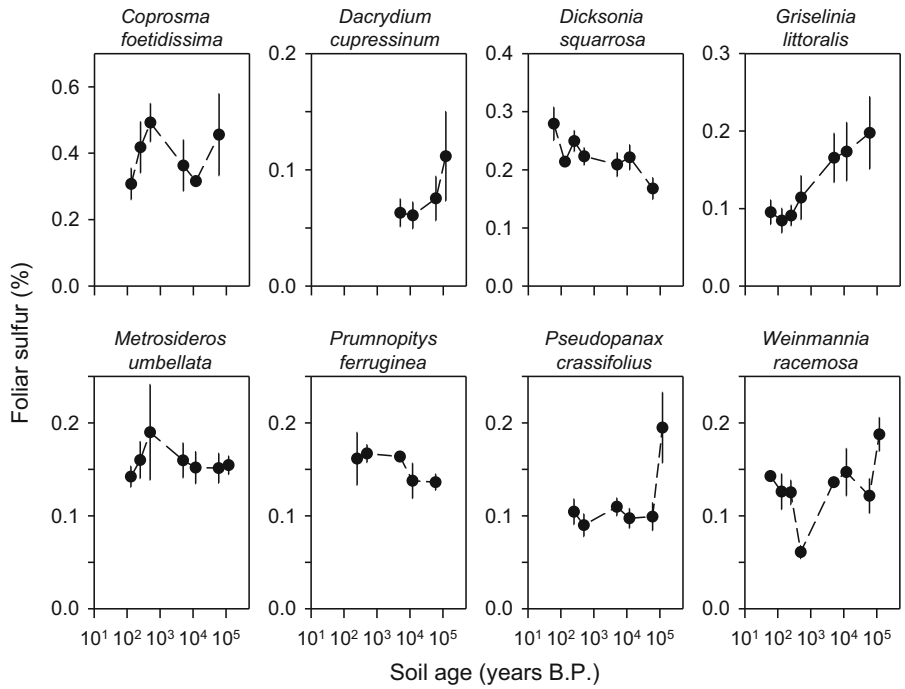

Fig. 5 Foliar sulfur (S) concentrations in eight plant species along the 120,000 year Franz Josef post-glacial chronosequence, New Zealand. Values are the mean ± standard error of between two and five individuals of each species at each site. Note differences in the *Y* axis scales among species

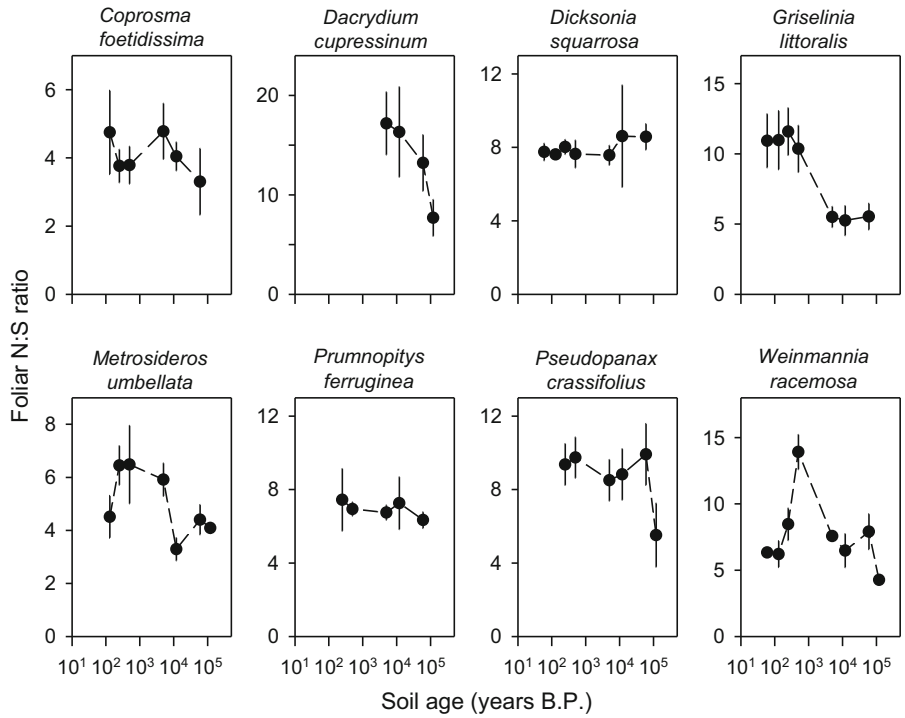

Fig. 6 Ratios of total nitrogen (N) to total sulfur (S) in leaves of eight plant species along the 120,000 year Franz Josef post-glacial chronosequence, New Zealand. Values are the mean ± standard error of between two and five individuals of each species at each site. Note differences in the *Y* axis scales among species

significantly along the chronosequence, although foliar P:S declined significantly (Supplementary Table 2).

Sulfur K-Edge XANES spectroscopy of organic sulfur in NaOH extracts

Spectra from XANES spectroscopy of extracts of mineral and organic horizons are shown in Fig. 8. The majority of the extracted organic S was C-bonded, representing between 63 and 77 % of the total extracted S in mineral soils and between 60 and 76 % of the total in the organic horizon (Table 3; Fig. 9a; Supplementary Table 3). Carbon-bonded S occurred in approximately equal proportions of highly-reduced and intermediate oxidation states; for example, mean proportions in the organic horizon across the sequence were 33.6 ± 4.0 % in highly-reduced forms and 33.1 ± 3.3 % in intermediate oxidation states (Table 3). The corresponding values for mineral soils were 34.0 ± 4.0 % in highly-reduced forms and 38.4 ± 3.0 % in intermediate oxidation states.

Ester-bonded S varied between 23 and 30 % of the extracted S in mineral soil across the majority of the chronosequence and showed no clear pattern during ecosystem development (Fig. 9b, Table 3). However, it accounted for 37 % of the extracted S in the 1000 year soil. In the organic horizon, ester-bonded S accounted for 24 % of the total extracted S in the 60 year old soil (which also had the lowest C:N ratio) and then increased to between 30 and 40 % for the remainder of the chronosequence. In general, there was little variation in organic S composition between mineral and organic horizons, although the organic horizon contained a slightly smaller proportion of S in intermediate oxidation states, and a slightly greater proportion of ester-bonded S than the mineral horizon (Table 3).

Highly reduced S accounted for between 28 and 40 % of the total extracted S in both mineral and organic horizons, but did not vary consistently with soil age (Fig. 9c). Most of the highly reduced S

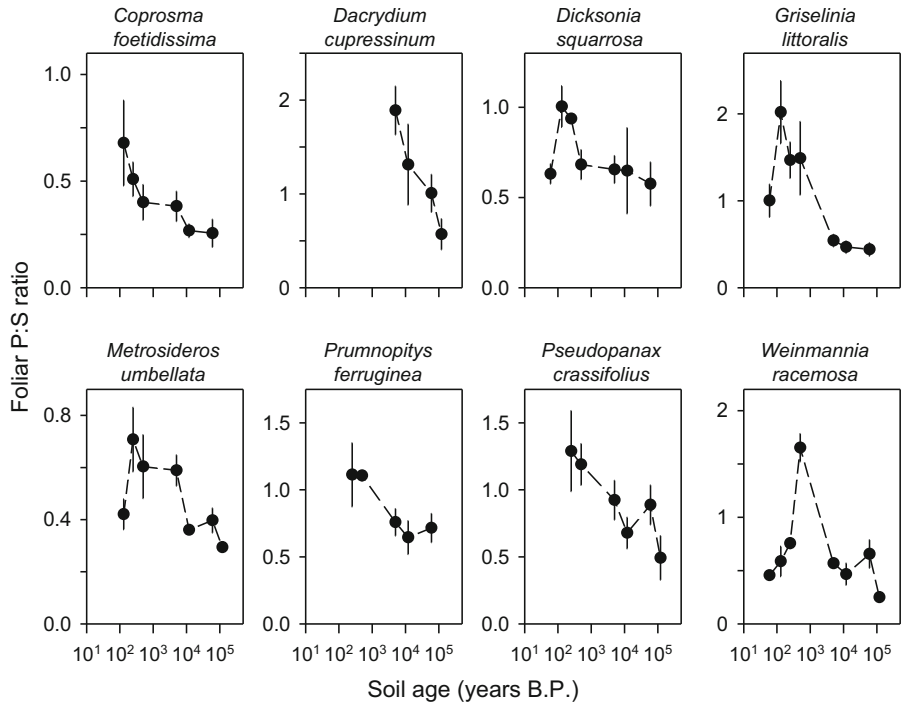

Fig. 7 Ratios of total phosphorus (P) to total sulfur (S) in leaves of eight plant species along the 120,000 year Franz Josef post-glacial chronosequence, New Zealand. Values are the mean ± standard error of between two and five individuals of each species at each site. Note differences in the *Y* axis scales among species

occurred as thiols and organic sulfides (i.e. Gaussian group 1; mean 20.1 ± 2.3 % in mineral soils and 21.9 ± 2.3 % in the organic horizon), with smaller proportions as thiophenes (i.e. Gaussian group 2; mean 13.9 ± 2.6 % in mineral soils and 11.7 ± 2.6 % in the organic horizon) (Table 3).

Sulfur in intermediate oxidation states declined in mineral soil throughout the chronosequence, from 42.3 % of the total extracted S in the 60 year old soil to 35.1 % in the 120,000 year old soil (Fig. 9d). This pool of S did not, however, vary consistently with time in the organic horizon (27–38 % of total extracted S). A greater proportion of the S in intermediate oxidation states occurred as sulfonates (i.e. Gaussian group 4; mean 22.9 ± 2.9 % in mineral soil and 20.7 ± 1.1 % in the organic horizon) compared to sulfoxides (i.e. Gaussian group 3; mean 15.5 ± 2.7 % in mineral soils and 12.5 ± 2.9 % in the organic horizon) (Table 3).

The NaOH–NaF extraction does not recover the total soil S, even though the majority of the soil S is likely to be in organic forms throughout the chronosequence (Freney and Williams 1983). However, multiplying the proportional data from XANES spectroscopy with the total soil S concentrations determined by elemental analysis allows estimation of changes in the concentrations of soil organic S forms along the chronosequence (Supplementary Fig. 1). In the organic horizon, only ester-sulfate showed a clear pattern along the chronosequence, increasing markedly in young soils and declining in old soils (Supplementary Fig. 1a). Concentrations of other S forms (sulphoxides, sulphonates, highly reduced S) fluctuated along the sequence, but all three forms declined in old soils. In contrast, all S forms in mineral soils increased in the first 1000 years and then declined in older soils (Supplementary Fig. 1b).

Ratios of S groups have proved useful in detecting soil organic S dynamics in previous studies, but showed few clear patterns along the Franz Josef chronosequence (Supplementary Fig. 3). The ratio of C-bonded S to ester-bonded S was high in the 60 year old organic horizon, perhaps reflecting the predominance of relatively undecomposed organic matter, and then declined and remained relatively stable at approximately 2.0 for the remainder of the chronosequence

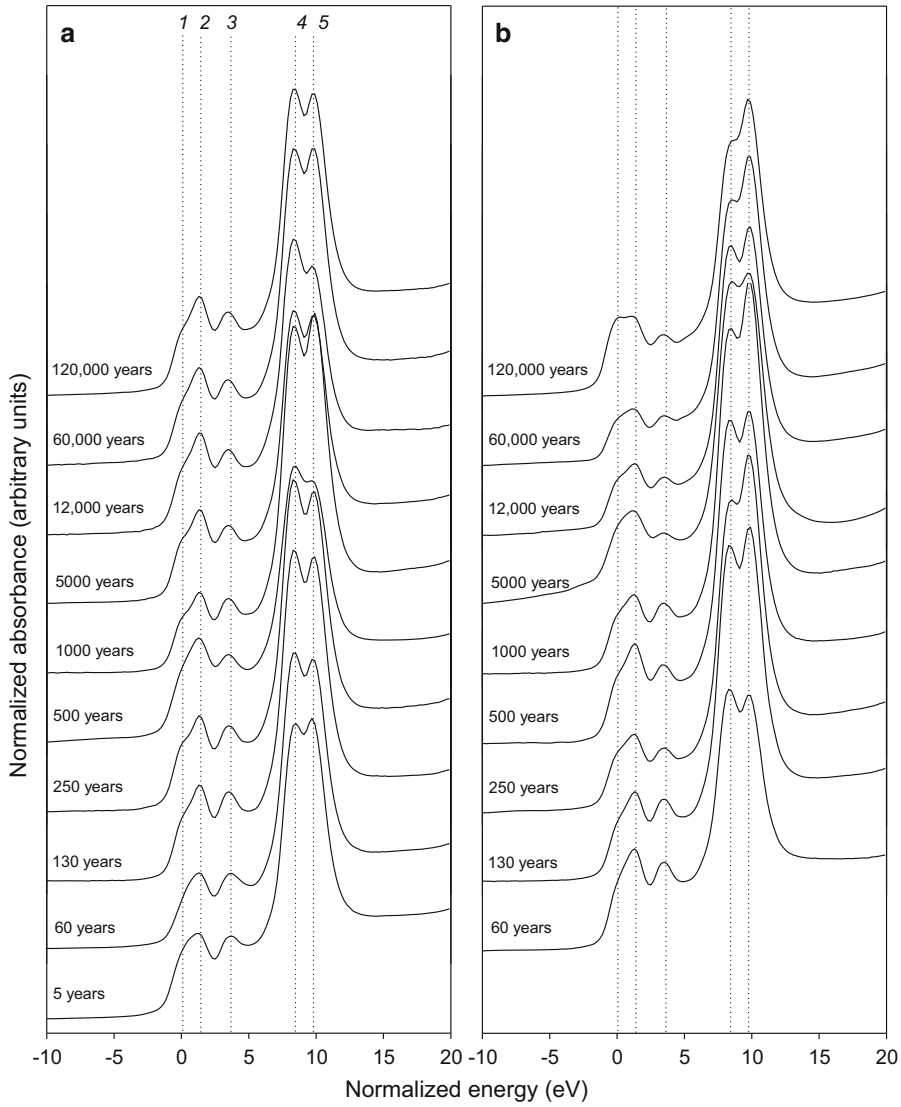

Fig. 8 Sulfur *K*-edge XANES spectra of NaOH–NaF extracts of mineral soil (**a**) and the organic horizon (**b**) along the 120,000 year Franz Josef post-glacial chronosequence, New Zealand. *Dashed lines* at the *top* of *panel* (**a**) indicate the positions of Gaussian curve (GC) 1 (thiols, organic sulfides), GC 2 (thiophenes), GC 3 (sulfoxides), GC 4 (sulfonates), and GC 5 (ester sulfates) (see Table 3)

(Supplementary Fig. 2a). The ratio of intermediate-oxidation S to ester-bonded S showed a similar pattern (Supplementary Fig. 2b). Both ratios were greater overall in mineral compared to the organic horizon (Table 3). However, the ratio of oxidized to reduced S and the decomposition index both varied little along the sequence or between mineral and organic horizons (Supplementary Fig. 2c, d).

Soil sulfatase activity and enzyme stoichiometry

We previously published data on sulfatase activity expressed on the basis of dry soil (Allison et al. 2007), whereby sulfatase increased in mineral soils from 8.9 ± 0.7 nmol MU g^{-1} h^{-1} in the young 60 year old soils to a maximum of 27.5 ± 6.2 nmol MU g^{-1} h^{-1} in the 500 year old soil, before stabilizing at 18–20 nmol MU g^{-1} h^{-1} in mature soils (12,000–120,000 years). In the organic horizon, sulfatase activity was extremely high in the youngest soil (124.7 ± 17.1 nmol g^{-1} h^{-1}), increased from 37.1 ± 3.8 nmol g^{-1} h^{-1} in 130 year soils to 67.1 ± 11.4 nmol g^{-1} h^{-1} on 1000 year old soils, and then declined continuously to lower rates of activity in the oldest soils (~28 nmol g^{-1} h^{-1} in 60,000–120,000 year old soils).

Standardization of sulfatase activity by soil C concentration revealed a consistent pattern of activity

Table 3 Mean values for functional organic sulfur (S) groups determined by S *K*-edge XANES spectroscopy of organic S extracted in NaOH–NaF from mineral soil and organic horizons along the 120,000 year Franz Josef post-glacial chronosequence, New Zealand

Sulfur group	Gaussian curve[a]	Formula	Oxidation state	Organic horizon (%)	Mineral horizon (%)
Thiols[b], organic sulfides	G1	R–SH, R–S–R′	0.14–0.38	21.9 ± 2.3	20.1 ± 2.3
Thiophenes[c]	G2	S in aromatic rings	0.80–0.96	11.7 ± 2.6	13.9 ± 2.6
Sulfoxides[d]	G3	R–SO–R′	1.25–1.82	12.5 ± 2.9	15.5 ± 2.7
Sulfonates	G4	R–SO_2O–H	5.00	20.7 ± 1.1	22.9 ± 2.3
Ester sulfates	G5	R–O–SO_3–H	6.00	33.3 ± 4.8	27.5 ± 4.3
Carbon-bonded S (G1 + G2 + G3 + G4)			≤5.0	66.7 ± 4.8	72.5 ± 4.3
Highly reduced S (G1 + G2)			<1.0	33.6 ± 4.0	34.0 ± 4.0
Intermediate oxidation states (G3 + G4)			1.0–5.0	33.1 ± 3.3	38.4 ± 3.0
Carbon-bonded: ester				2.1 ± 0.5	2.7 ± 0.5
Oxidized: reduced				2.0 ± 0.4	2.0 ± 0.4
Intermediate oxidation: highly oxidized				1.0 ± 0.3	1.4 ± 0.2
Decomposition index[e]				1.2 ± 0.23	1.0 ± 0.3

Values are the proportion (%) ± standard deviation of the total extracted S (i.e. approximating the total soil S) averaged across the nine sites along the chronosequence in which XANES spectroscopy was used (excluding the youngest site). Each sample represented a composite sample of five replicate plots at the site

[a] Derived from spectral analysis in S *K*-edge XANES spectroscopy

[b] Thiols contain a carbon-bonded sulfhydryl (SH) group

[c] Thiophenes are heterocyclic aromatic compounds

[d] Sulfoxides contain a sulfonyl group (SO) and are the oxidized derivatives of sulfides

[e] Decomposition index is based on changes in S groups during litter decomposition (Schroth et al. 2007) and is defined as sulfonates and sulfates (G4 + G5)/sulfides and sulfoxides (G1 + G2 + G3)

in both mineral and organic horizons (Fig. 10a). When expressed on the basis of soil C, sulfatase activity in mineral soils was initially high in the youngest soil (0.80 ± 0.05 nmol MU mg^{-1} C h^{-1}) and then declined to relatively low values in older soils between 5000 and 120,000 years old (0.20–0.28 nmol MU mg^{-1} C h^{-1}). Similarly, activity was initially high in the organic horizon (0.68 ± 0.06 nmol MU mg^{-1} C h^{-1}) and declined to low values in older soils (0.14–0.19 nmol MU mg^{-1} C h^{-1}), although there was a peak at approximately 0.4 nmol MU mg^{-1} C h^{-1} after 1000 years, presumably representing a temporary increase in S demand.

The ratio of phosphomonoesterase to sulfatase increased continuously throughout the chronosequence in both mineral and organic horizons (Fig. 10b). In both cases, the ratio increased from <35 in young soils to >250 in the oldest soils. In contrast, the ratios of C (β-glucosidase) and N (*N*-acetyl β-glucosaminidase) enzymes to sulfatase showed no clear trends along the chronosequence for either mineral or organic horizons (Fig. 10c, d). However, the ratios were always greater in the organic horizon than in the mineral soil.

Stable S isotope ratios ($\delta^{34}S$) in soils

In mineral soil, $\delta^{34}S$ increased gradually throughout the chronosequence, increasing from a minimum of 14.3 ± 0.38 ‰ in the 130 year old soil to between 19.9 and 20.7 ‰ in ≥12,000 year old soils (Fig. 11a). The initial increase was more pronounced in the organic horizon, in which $\delta^{34}S$ increased from 6.0 ± 0.60 ‰ in 60 year old soil to 20.6 ± 0.30 ‰ in the 120,000 year old soil (Fig. 11b). However, the $\delta^{34}S$ of the organic horizon varied little after about 500 years of pedogenesis.

Discussion

Sulfur is an important macronutrient, but its behavior during long-term ecosystem development is poorly understood in comparison with N and P. Indeed, only a

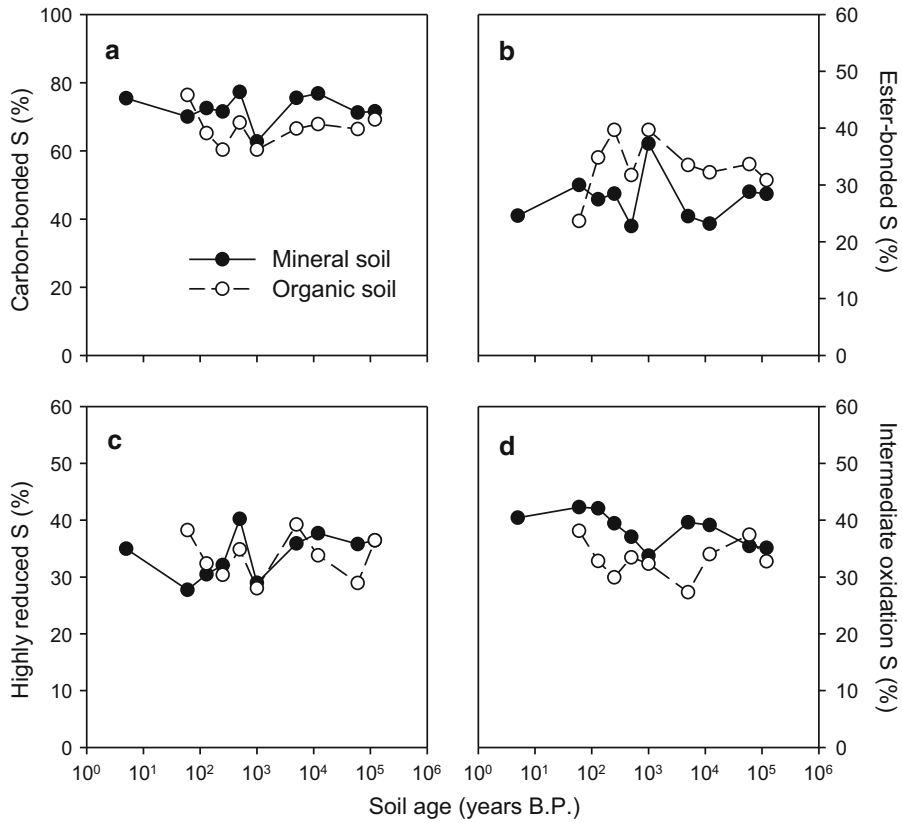

Fig. 9 The chemical nature of organic sulfur (S) determined by S *K*-edge XANES spectroscopy in NaOH–NaF extracts of mineral soil (*filled symbols* and *solid line*) and the organic horizon (*open symbols* and *dashed line*) along the 120,000 year Franz Josef post-glacial chronosequence, New Zealand. The figure shows carbon-bonded S (**a**), ester-bonded S (**b**), highly-reduced S (**c**), and S in intermediate oxidation states (**d**). Values are the proportion (%) of the total extracted S, which approximates the total soil S in all except the youngest (5 year) soil, from analysis of a composite sample of five replicate plots at each site

few studies have reported S concentrations or dynamics along soil chronosequences (Syers et al. 1970; Jehne and Thompson 1981; Prietzel et al. 2013; Bern et al. 2015). The Franz Josef chronosequence offers an opportunity to study long-term S dynamics in a region unaffected by anthropogenic S deposition. We hypothesized that changes in S demand during ecosystem development would be reflected in changes in S concentrations and stoichiometry in soils and leaf tissue, sulfatase activity and enzyme stoichiometry in soils, stable S isotopes, and the chemical composition of soil organic S. However, other than an initial period of high S demand in very young soils, we found little evidence for significant change in the S cycle during 120,000 years of ecosystem development.

Atmospheric sulfur inputs

Although the chronosequence is unaffected by pollutant S deposition, it receives modest inputs of atmospheric S from oceanic sources, estimated here to be 5.4–8.7 kg S ha^{-1} $year^{-1}$ depending on rainfall and distance to the coastline. These rates of S deposition are comparable to current total S deposition rates in much of Europe, Asia, and eastern North America, which receive between 4 and 20 kg S ha^{-1} $year^{-1}$, with some areas receiving >40 kg S ha^{-1} $year^{-1}$. Results from the current study are therefore broadly generalizable for sites receiving moderate amounts of S deposition. Since temperate forests typically require <5 kg S ha^{-1} $year^{-1}$ to support growth (Johnson 1984), it seems unlikely that primary productivity is limited by S availability at any stage of the Franz Josef chronosequence. The similarity in atmospheric S deposition along the chronosequence, particularly in the early stages (i.e., <5000 years), suggests that changes in S dynamics along the sequence can be attributed primarily to variation in biogeochemical cycling related to ecosystem development rather than differences in S inputs from the atmosphere.

Soil sulfur concentrations and stoichiometry

Most mineral soils contain total S concentrations between 50 and 800 mg S kg^{-1} (i.e., 0.005–0.080 %), whereas forest floor or organic horizons contain total S

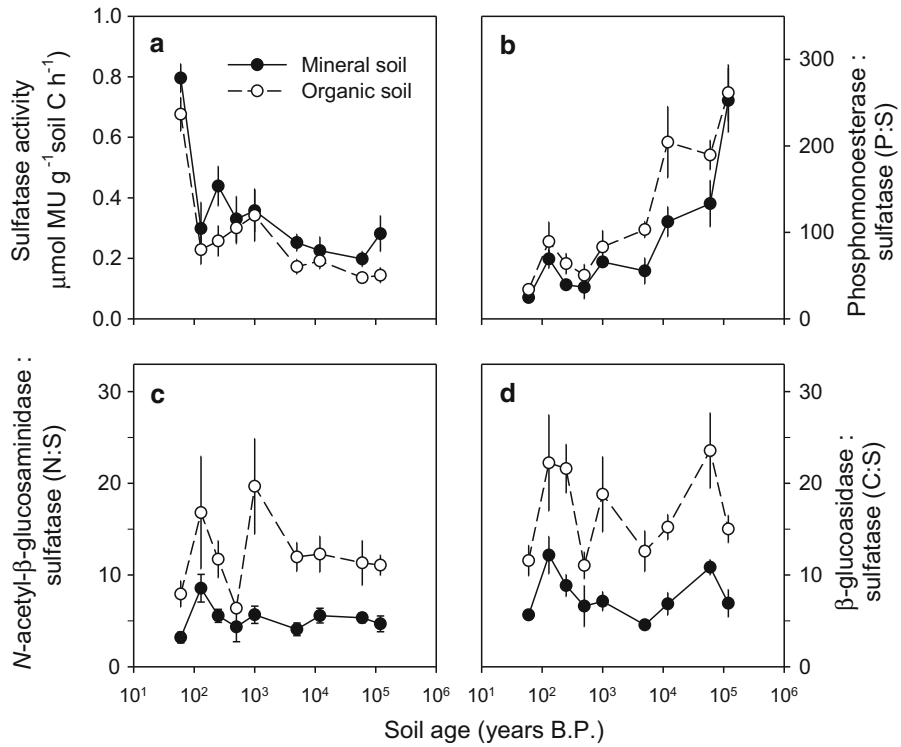

Fig. 10 Sulfatase activity in mineral soil (*filled symbols* and *solid line*) and the organic horizon (*open symbols* and *dashed line*) along the 120,000 year Franz Josef post-glacial chronosequence, New Zealand (**a**) and the ratios of phosphomonoesterase to sulfatase (i.e. phosphorus to sulfur (S) enzymes) (**b**), *N*-acetyl-β-glucosaminidase to sulfatase (i.e. nitrogen (N) to S enzymes) (**c**), and β-glucosidase to sulfatase (i.e. carbon (C) to S enzymes) (**d**). Sulfatase activity is expressed as µmol of methylumbelliferol released per g of soil C per hour

concentrations between 1000 and 2000 mg S kg^{-1} (i.e., 0.1–0.2 %) (Freney and Williams 1983; Mitchell et al. 1992; Zhao et al. 1996; Lambert and Turner 1998). Soil S concentrations during 120,000 years of pedogenesis along the Franz Josef chronosequence therefore span the range of S in mineral and organic horizons worldwide.

As expected, soil S concentrations were closely correlated with the concentrations of total C and N, reflecting the fact that the majority of soil S occurs in organic forms (Freney and Williams 1983). The exception was the youngest mineral soil (5 years old), which presumably contained a significant concentration of inorganic S in primary minerals. Primary mineral S disappears within the first few years of pedogenesis (Prietzel et al. 2013), so it seems likely that the soil S was predominantly in organic form throughout the remainder of the Franz Josef chronosequence.

The stoichiometry of C, N, and S in organic matter is relatively well-constrained in ecosystems worldwide, with global means of approximately 100 for C:S and 7.7 for N:S (Freney and Williams 1983). However, there appears to be greater variation in C:S than in N:S, as demonstrated by results from the Franz Josef chronosequence. For a range of Southern Hemisphere mineral soils under a variety of climates, N:S ratios were mostly between 7 and 10, although values ranged from 4.7 on granite in Ghana to 22.5 on sand in Australia (Lambert and Turner 1998). More recently, C:N:S ratios of 100:8.3:1.4 were reported for a global dataset (i.e. C:S about 70 and N:S about 6), with similar values for a range of Australian soils (Kirkby et al. 2011). For a series of New Zealand grassland soils, C:N:S ratios in the upper 50 cm averaged 120:10:1.3 (i.e. C:S about 100 and N:S about 8) (Walker and Adams 1958). However, for a weathering sequence of New Zealand soils developed in greywacke, the N:S ratio was 9.1 in weakly weathered soils, 8.3 in moderately weathered soils, and 7.7 in strongly-weathered soils, even though the C:S ratio was relatively constant across sites (150–159) (Walker and Adams 1959). Compared to the global average, the ratios reported here for the Franz Josef chronosequence are therefore relatively high for both C:S (Franz Josef mean 181 ± 31 and 198 ± 37 for mineral and organic horizons, respectively) and N:S (9.1 ± 0.7 and 8.0 ± 0.9 for mineral and organic

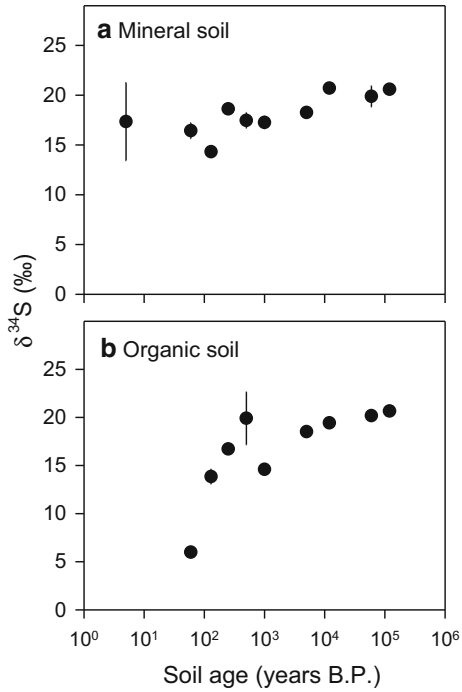

Fig. 11 Stable S isotope ratios ($\delta^{34}S$) in mineral soil (**a**) and the organic horizon (**b**) along the 120,000 year Franz Josef post-glacial chronosequence, New Zealand. Values are the mean ± standard error of five replicate plots at each site

horizons, respectively), but are similar to other New Zealand soils, at least for N:S. This suggests that S availability is relatively low along the entire Franz Josef chronosequence and elsewhere in New Zealand, despite the annual input of 5–8 kg S ha^{-1} from the atmosphere, which exceeds the typical S requirement of temperate forest (Johnson 1984). A possible explanation is that the high precipitation at Franz Josef (4000–7500 mm $year^{-1}$) causes rapid and substantial loss of S from the system by leaching (see below).

The increase in the C:S ratio in the oldest soils at Franz Josef (60,000–120,000 years), exceeding 200 in both mineral and organic horizons, might indicate reduced S availability, P limitation of S acquisition by plants, or increasing conifer abundance (leaves of the dominant tree species *Dacrydium cupressinum* contained a relatively low S concentration and high N:S ratio and presumably C:S ratio; see below). Sulfur availability might be reduced in the two oldest sites because they receive approximately 4000 mm of annual precipitation and contain relatively low amorphous metal concentrations (Turner et al. 2007), meaning that they have a much lower potential to retain atmospheric S against losses by leaching. Sulfur limitation seems unlikely, however, because inputs from the atmosphere are relatively high at the three oldest sites, sulfatase activities in the soil do not increase in the oldest soils, and foliar S is relatively high for most species in the oldest sites. A possible explanation for the increasing soil C:S ratio in the oldest soils is the increasing ratio of fungal to bacterial biomass along the Franz Josef chronosequence (Allison et al. 2007), because the C:S ratio appears to be greater for fungi compared to bacteria (Kirkby et al. 2011).

Soil P:S ratios in organic matter (i.e. organic P to total S) were about 1.4 for a global dataset (Kirkby et al. 2011), but considerably lower (about 0.5) for 22 New Zealand grassland soils (Walker and Adams 1958). At Franz Josef, P:S ratios in soils declined continuously throughout the chronosequence, from values greater than the global average in young soils to values considerably below the global average in old soils. The strong decline in soil P at Franz Josef is well-understood (Walker and Syers 1976; Richardson et al. 2004), but the declining P:S ratio indicates a corresponding increase in relative S availability during ecosystem development. This supports evidence from sulfatase activity (Allison et al. 2007; see below) and studies of bacterial S genes elsewhere (Schmalenberger and Noll 2010), which indicate that S availability is relatively low compared to P in the youngest soils, but that P availability decreases continually relative to S as pedogenesis proceeds.

Few studies have quantified changes in soil S along long-term chronosequences. Along the Hawaiian Island chronosequence, soil S in surface organic horizons was approximately 0.2 % between 300 and 4.1 million years of ecosystem development (Bern et al. 2015). For the 500,000 year dune chronosequence at Cooloola, Australia, total S concentrations in surface (0–10 cm) soils were approximately 0.002 % for the majority of the chronosequence, although they increased to 0.011 % in the oldest soils (Jehne and Thompson 1981). For the upper 1 m of soil along a wind-blown sand chronosequence at Manawatu in New Zealand, the C:S ratio in soil organic matter increased from low values initially (from 8 to 74 in the first 500 years of pedogenesis) to relatively stable values of >100 after 3000 years (Syers et al. 1970). The N:S ratio reached a maximum of 6.9 after

3000 years and then declined, while the P:S ratio in organic matter did not exceed 1.0 throughout the chronosequence. The relatively low N:S and P:S ratios at Manawatu and the relatively long time before the C:S ratio exceeded 100 (at Franz Josef this occurred after between 60 and 130 years) might reflect a greater rate of S loss in runoff under the high rainfall regime at Franz Josef (4000–7500 mm $year^{-1}$) compared to Manawatu (approximately 1000 mm per year).

For two young glacial foreland chronosequences, soil S concentrations increased rapidly within the first few decades of pedogenesis, as inorganic sulfides were depleted in surface mineral soils (within 75 years) and S accumulated in organic forms (Prietzel et al. 2013). Soil S concentrations peaked after about 50 years (0.23 % in the organic horizon and 0.14 % in the surface mineral soil) in the Hailuogou chronosequence in southwestern China, and after about 80 years (0.04 % in mineral soil) in the Damma chronosequence in Switzerland. We expect that depletion of inorganic S at Franz Josef occurred after even shorter periods of time, given the very high annual rainfall (7500 mm) in the upper part of the valley where the youngest soils occur.

In the glacial foreland chronosequences, S in surface mineral soils was correlated with amorphous metal oxides (Prietzel et al. 2013), suggesting their importance in regulating soil S dynamics during pedogenesis. Indeed, amorphous iron sorbs S strongly (Parfitt and Smart 1978). Both amorphous aluminum and iron oxide concentrations vary markedly along the Franz Josef chronosequence, increasing in young soils and declining strongly in old soils as the oxides ripen into crystalline forms (Turner et al. 2007). The changes in amorphous metal oxides along the Franz Josef chronosequence follow a similar pattern to total soil S concentrations, suggesting a potential control on soil S during pedogenesis.

Foliar S concentrations and elemental stoichiometry

Foliar S concentrations span a wide range in plants worldwide, with concentrations for optimal growth reported to be 0.1–0.5 % (Marschner 2006). For example, Lambert and Turner (1998) suggested that foliar S concentrations for *Pinus radiata* and *Eucalyptus maculata* under conditions of sufficient S were 0.11 % and 0.14–0.16 %, respectively. The eight plant species we studied along the Franz Josef chronosequence were generally within this range, although patterns of foliar S along the chronosequence varied inconsistently among species, including increases, decreases, and no change during ecosystem development. The lowest foliar S concentrations occurred in *Dacrydium cupressinum* (0.08 %), consistent with the relatively low foliar S in conifers compared to deciduous plants. For example, foliar S concentrations across Europe are typically lower in conifers (0.10 %; predominantly *Pinus sylvestris* and *Picea abies*) compared to deciduous species (0.19 %) (Reimann et al. 2003). However, the other southern conifer in our dataset, *Prumnopitys ferruginea*, contained a similar foliar S concentration to the angiosperms.

The highest foliar S concentrations occurred in *Coprosma foetidissima* (mean 0.39 %). This is at the upper end of the range of foliar S concentrations (0.14–0.39 %) reported for ten *Coprosma* species growing on soils derived from loess or basalt near Dunedin, New Zealand (Lee and Johnson 1984), although a foliar S concentration of 0.49 % was reported for *C. foetidissima* growing in the subantarctic Auckland Islands (Lee 1988). *Coprosma foetidissima* is known for its foul smell, which has been attributed to methanethiol (CH_4S) (Sutherland 1947). Volatile S compounds such as methanethiol appear to function as an attractant for insects (Hell and Kruse 2007), but in this case do not seem to act as a defense against mammalian herbivores, given that *C. foetidissima* is not particularly unpalatable (Forsyth et al. 2002).

Sulfur occurs in plant tissue predominantly as amino acids, so there is typically a strong relationship between N and S in leaves. However, foliar N:S is responsive to changes in S availability and can therefore be used to indicate the demand for S relative to the demand for N. When S is in adequate supply it can accumulate in non-protein forms, resulting in a decrease in the foliar N:S ratio. In contrast, insufficient S can limit protein formation, leading to an accumulation of N and an increase in the foliar N:S ratio (Lambert and Turner 1998). Such changes might occur during ecosystem development. For example, if P availability limits N fixation during long-term pedogenesis then foliar N:S should decline. Here, foliar N:S ratios varied widely among species (species means 4.1–13.6), but the ratios for individual species were relatively stable along the chronosequence. The

greatest N:S ratios were in the conifer *D. cupressinum*, consistent with values of 14.4 (mass basis) reported previously for conifer leaves that did not contain inorganic S (Kelly and Lambert 1972). Based on this, and the N:S ratio of amino acids in plant tissue, it can be assumed that a foliar N:S ratio <14 indicates S sufficiency, and a ratio >14 indicates S deficiency (i.e. molar ratio of 33) (Dijkshoorn and van Wijk 1967; Lambert and Turner 1998). Thus, we infer that no species at Franz Josef was S deficient along the chronosequence, except perhaps for *D. cupressinum* in intermediate aged soils. However, foliar N:S did decline for several species in the late stages of ecosystem development, suggesting an increase in S availability relative to N on older soils. Foliar P:S ratios also varied markedly among species, but declined continuously along the chronosequence. This supports the continual decline in P availability during pedogenesis at Franz Josef, and greater demand for S relative to P in younger soils (see above).

Sulfatase activity and enzyme stoichiometry

In natural ecosystems that are little affected by atmospheric pollution and with S-poor bedrock, the supply of S to organisms is regulated predominantly by recycling of organic matter by the soil microbial biomass (Maynard et al. 1984; Zhao et al. 1996). Plants take up S as inorganic sulfate from the soil, so the activity of sulfatase enzymes and the release of inorganic sulfate through hydrolysis of ester-bonded S is a key step in the soil S cycle (Bünemann and Condron 2007).

Previously, we reported the activity of sulfatase and other enzymes along the Franz Josef chronosequence on a soil mass basis (Allison et al. 2007), which indicated an increasing investment in P acquisition as ecosystem development proceeds, consistent with the concept of strengthening P limitation of biological productivity. However, results for the early stages of pedogenesis were unclear, because sulfatase activity was high in the young organic horizon but not in young mineral soil. Here we recalculated this enzyme data on a per soil C basis, and report changes in 'enzymatic stoichiometry' along the chronosequence—i.e. the ratios of enzymes involved in the acquisition of C, N, and P from organic compounds to sulfatase activity. This is assumed to reflect the relative investment by microorganisms in the acquisition of different nutrients (Sinsabaugh et al. 2009), although it has not been examined widely for sulfatase. When expressed on a per C basis, sulfatase activity was highest in both the youngest mineral and organic horizons, revealing a consistent strong belowground S demand in the earliest stages of pedogenesis. Low S availability in young soils was also shown in a study of a glacial forefield chronosequence in Switzerland that found a high diversity of desulfonating bacteria (Schmalenberger and Noll 2010). These included taxa characteristic of low S environments, indicating that S availability is a limiting factor to microbial growth in very young soils.

After the high initial activity on young soils, sulfatase activity decreased markedly and continued to decline in older soils, consistent with increasing S availability as ecosystem development proceeds. Together with the continual increase in the enzymatic P:S ratio along the chronosequence in both mineral and organic horizons, this indicates a gradual decline in microbial investment in S acquisition compared to P acquisition, consistent with a continual increase in P demand during long-term pedogenesis. The greater ratio of β-glucosidase and *N*-acetyl β-glucosaminidase to sulfatase in mineral soils compared to organic horizons indicates a greater relative demand for S in mineral soil, consistent with greater C:S and N:S ratios in mineral soil than the organic horizon. However, sulfatase did increase slightly in intermediate-aged soils at Franz Josef, in parallel with a decline in the β-glucosidase to sulfatase ratio. This suggests a short period of greater belowground S demand after approximately 500 years of ecosystem development, when both N and P are present in relatively high concentrations. The pattern is not related to differences in atmospheric S inputs, given the similarity in deposition rates at sites spanning the initial 5000 years of pedogenesis (Table 1).

Stable sulfur isotope ratios

Soil $\delta^{34}S$ values vary from −30 to +30 ‰ at the global scale, linked to differences in atmospheric and geological inputs of S to the ecosystem (Krouse et al. 1991). Soil $\delta^{34}S$ can vary due to changes in pollutant S inputs (Bol et al. 2005), although the negligible anthropogenic S deposition onto the west coast of the South Island of New Zealand (Vet et al. 2014) means that this does not influence soil $\delta^{34}S$ along the

Franz Josef chronosequence. A recent study examined changes in $\delta^{34}S$ along the Hawaiian Islands chronosequence (Bern et al. 2015). In general, soil and plant $\delta^{34}S$ decreased with increasing elevation, annual rainfall, and proximity to the coastline, reflecting a balance between marine and volcanic sources in atmospheric S deposition. Along the chronosequence at 2500 mm annual rainfall, $\delta^{34}S$ increased continuously from relatively low values (0 to +2.7 ‰) on young soils (300 years) to between +17.8 and +19.3 ‰ on old soils (4.1 million years). However, it was not possible to attribute changes in $\delta^{34}S$ to pedogenesis or ecosystem development, because the isotopic signature of the parent basalt was similar to that of volcanic aerosols, and the contribution of both these sources declined with increasing island age.

At Franz Josef, $\delta^{34}S$ in the organic horizon increased markedly from relatively low value (+6 ‰) at the youngest site (60 years old) to around +20 ‰ in the older soils. Most of the variation occurred in the early stages of the chronosequence, so it is unlikely that this is due to variation in atmospheric S input, because input rates are similar for sites spanning the first 5000 years of ecosystem development. The relatively low $\delta^{34}S$ in the organic soil of the young site (+6 ‰) is much lower than values from marine sources (+16 ‰ for marine biogenic S and +21 ‰ for sea salt) and therefore suggests the signature of primary mineral S from bedrock weathering. Paradoxically, however, $\delta^{34}S$ of the surface mineral soil in both the 5 and 60 year old sites was much higher (+16 ‰) than that in the 60 year old organic horizon. A possible explanation is that the surface mineral soil (0–10 cm) was leached of bedrock S, even after 5 years (although there was considerable variation among replicates in the youngest soil), and that the low $\delta^{34}S$ of the organic soil reflects plant uptake of rock-derived S from deeper parts of the soil profile that were not leached of primary mineral S. Indeed, foliar $\delta^{34}S$ for one of the few species on the 60 year old site, *Griselinia littoralis*, was also low (+1.8 ± 1.0 ‰, unpublished data). A study of tropical soils in Costa Rica showed that only very young soils retained the $\delta^{34}S$ signature of the bedrock (Bern and Townsend 2008) and a rapid decline in primary mineral sulfate was also found in two glacial foreland chronosequences (Prietzel et al. 2013). The extremely high annual precipitation at the youngest sites along the Franz Josef chronosequence (7500 mm) might explain why the surface soils were already leached of primary mineral S at these locations.

In the older stages of the chronosequence, $\delta^{34}S$ increased to approximately +20 ‰ in both mineral and organic horizons. This might reflect a loosening of the S cycle (i.e. greater fractionation) with strengthening P limitation, accumulation of atmospheric S (Bern and Townsend 2008), or the closer proximity to the coastline and therefore a greater similarity to SO_4^{2-} in sea water ($\delta^{34}S$ of approximately +21 ‰) (Kusakabe et al. 1976; Bern et al. 2015). The latter explanation appears most likely, because the three oldest sites probably receive a slightly greater proportion of their S inputs from sea spray (based on Fig. 2 in Ledgard and Upsdell 1991) compared to the younger part of the chronosequence, where S inputs are likely to be derived in approximately equal proportions from sea salt and marine biogenic sources.

Chemistry of soil organic sulfur along the chronosequence

Most S in plant tissue is in amino acids (principally cysteine and methionine), so S inputs to the soil surface in litter fall are predominantly as C-bonded S (Zhao et al. 1996). In contrast, most soils contain a mixture of C-bonded S, sulphonates, and ester-bonded S, reflecting microbial inputs and transformations of plant litter inputs (Solomon et al. 2003; Prietzel et al. 2007; Zhao et al. 1996). Sulfur in soil organic matter can be released via biological mineralization (i.e. oxidation of C-bonded S driven by a microbial demand for energy) or by biochemical mineralization (i.e. enzymatic hydrolysis of ester-bonded S driven by a microbial demand for S).

Based on the McGill and Cole (1981) model, we hypothesized that changes in S availability would be reflected in the balance between ester-bonded and C-bonded S. However, despite major changes in total soil S along the Franz Josef chronosequence, we detected relatively little variation in its chemical nature, particularly given the relatively large changes that have been observed following land use change (e.g., Solomon et al. 2003, 2009; Zhao et al. 2006). Soil organic S at Franz Josef was dominated by C-bonded S, distributed approximately equally between highly reduced and intermediate oxidation states, although ester-bonded S accounted for a

considerable proportion of the total organic S (30–40 %). There was relatively little difference between mineral and organic horizons, as reported for northern hardwood forests in the USA (Schroth et al. 2007), although ester-bonded S in the organic horizon increased rapidly in young soils and was a greater proportion of the S compared to the mineral soil for the majority of the Franz Josef chronosequence. This perhaps reflects the relatively abundance of fungi in the organic horizon, which can contain a large proportion of their S in ester-bonded form (Zhao et al. 1996). However, we observed no clear temporal variation in the ratio of C-bonded to ester-bonded S that might indicate a shift in S demand or turnover during ecosystem development.

Only one previous study has examined changes in soil organic S composition along soil chronosequences. Prietzel et al. (2013) used XANES spectroscopy on solid samples to assess the total soil S in glacial forelands chronosequences at the Hailuogou glacier in southwestern China (120 years old) and the Damma glacier in Switzerland (>700 years old). There were rapid changes in soil S chemistry along both chronosequences, as inorganic sulfides in the parent rock were oxidized within 30 and 75 years, respectively. This decline in inorganic S presumably occurred even more rapidly under the wet, warm climate at Franz Josef (our first site for XANES spectroscopy was 60 years old). Organic S in the glacial forefield chronosequences was dominated by S with electron oxidation states greater than +1.5 (i.e. sulphoxides, sulphones, sulphonates, and ester sulfate), yielding oxidized-S to reduced-S ratios of >1 for all sites (Prietzel et al. 2013). Similarly, the oxidized to reduced S ratios at Franz Josef were >1 throughout the chronosequence.

We did not quantify microbial S along the chronosequence. Microbial S typically constitutes only a small proportion (<3 %) of the total S in most soils (e.g., Wu et al. 1994), but might be of greater quantitative importance at Franz Josef, particularly in the organic horizon (Chen et al. 2001), given that the microbial biomass contains up to 29 % of the soil organic P along the chronosequence (Turner et al. 2013). Microbial S occurs mainly as amino acids, although fungi can contain a large proportion of their S in ester-bonded form, probably as choline sulfate (Zhao et al. 1996). If the microbial biomass accounts for a comparable proportion of the soil organic S as it does for soil organic P, this could conceivably influence the soil S speciation along the chronosequence.

Synthesis

Despite its importance as a plant macronutrient, few studies have examined S dynamics during long-term ecosystem development. The Franz Josef chronosequence provides an important opportunity to study S dynamics during long-term ecosystem development in an environment that has not been affected by anthropogenic S deposition from the atmosphere.

We hypothesized that changes in S demand during ecosystem development would be reflected in changes in S concentrations and stoichiometry in soils and leaf tissue, sulfatase activity and enzyme stoichiometry in soils, stable S isotopes, and the chemical composition of soil organic S. We found evidence that S demand was greatest in the youngest soils, with high sulfatase activity and narrow ratios of C, N, and P degrading enzymes to sulfatase. This high S demand in the very earliest stages of pedogenesis appeared to be driven by the rapid depletion of primary mineral S from surface mineral soils in in the high rainfall environment of the glacier forefield, and might influence rates of biological N fixation and therefore ecosystem productivity in the early stages of ecosystem development. Stable isotope ratios ($\delta^{34}S$) indicate that organisms continued to acquire and recycle rock-derived S from deeper parts of the soil profile after 60 years of pedogenesis, with a subsequent shift to predominantly atmospheric inputs on older soils along the chronosequence.

The Franz Josef chronosequence receives modest amounts of S input from the atmosphere (5–8 kg S ha^{-1} $year^{-1}$), which should be sufficient to support the growth of forests (Johnson 1984). Together with the strong relationship between C, N, and S in soil organic matter, the relatively minor changes in the chemical nature of organic S, and the relatively low sulfatase activity in all but the youngest soils, we conclude that S is probably in adequate supply in all but the youngest soils of the chronosequence, and that S turnover is controlled primarily by biological mineralization (i.e. driven by the demand for energy) rather than biochemical mineralization (i.e. driven by a demand for S). However, the temperate climate and high annual precipitation (4000–7500 mm) suggest that substantial S leaching

might drive rapid loss of primary mineral S in young soils, reduce the accumulation of S during long-term ecosystem development, and maintain moderate S availability relative to demand throughout the chronosequence.

Acknowledgments We thank Roger Cresswell for analytical support, Victoria Allison for assistance with sample collection, and Milton Solano and Ian Baillie for assistance in producing Fig. 1. The XANES measurements were supported by the National Research Initiative of the USDA–CSREES (2002-35107-122269). We thank W. Caliebe and S. Khalid for support during spectroscopic analyses. The XANES spectra were collected at the X-19A beam-line of the NSLS, Brookhaven National Laboratory, which is supported by the U.S. Department of Energy under the contract No. DE-AC02-76CH00016. Finally, we thank Carleton Bern and an anonymous reviewer for constructive criticism and insight that substantially improved the manuscript.

References

Allison VJ, Condron LM, Peltzer DA, Richardson SJ, Turner BL (2007) Changes in enzyme activities and soil microbial community composition along carbon and nutrient gradients at the Franz Josef chronosequence, New Zealand. Soil Biol Biochem 39:1770–1781

Almond PC, Moar NT, Lian OB (2001) Reinterpretation of the glacial chronology of South Westland, New Zealand. N Z J Geol Geophys 44:1–15

Bern CR, Townsend AR (2008) Accumulation of atmospheric sulfur in some Costa Rican soils. J Geophys Res 113:G03001

Bern CR, Chadwick OA, Kendall C, Pribil MJ (2015) Steep gradients of volcanic and marine sulfur in Hawaiian rainfall and ecosystems. Sci Total Environ 514:250–260

Bol R, Eriksen J, Smith P, Garnett MH, Coleman K, Christensen BT (2005) The natural abundance of ^{13}C, ^{15}N, ^{34}S and ^{14}C in archived (1923–2000) plant and soil samples from the Askov long-term experiments on animal manure and mineral fertilizer. Rapid Commun Mass Spectrom 19:3216–3226

Bünemann EK, Condron LM (2007) Phosphorus and sulphur cycling in terrestrial ecosystems. In: Marschner P, Rengel Z (eds) Nutrient cycling in terrestrial ecosystems. Soil biology, vol 10. Springer-Verlag, New York, pp 65–94

Chen CR, Condron LM, Davis MR, Sherlock RR (2001) Effects of land-use change from grassland to forest on soil sulfur and arylsulfatase activity in New Zealand. Soil Res 39:749–757

Coomes DA, Bentley W, Tanentzap A, Burrows L (2013) Soil drainage and phosphorus depletion contribute to retrogressive succession along a New Zealand chronosequence. Plant Soil 367:77–91

Dijkshoorn W, van Wijk L (1967) The sulphur requirements of plants as evidenced by the sulphur-nitrogen ratio in the organic matter. A review of published data. Plant Soil 26:129–157

Forsyth DM, Coomes DA, Nugent G, Hall GM (2002) Diet and diet preferences of introduced ungulates (Order: Artiodactyla) in New Zealand. N Z J Zool 29:323–343

Freney JR, Williams CH (1983) The sulfur cycle in soil. In: Ivanov MV, Freney JR (eds) The global biogeochemical sulphur cycle. Scientific Committee on Problems of the Environment (SCOPE) 19. Wiley, Chichester, pp 129–201

Gertheiss J (2014) ANOVA for factors with ordered levels. J Agric Biol Environ Stat 19:258–277

Haneklaus S, Bloem E, Schnug E (2007) Sulfur interactions in crop ecosystems. In: Hawkesford MJ, De Kok LJ (eds) Sulfur in plants—an ecological perspective. Springer, Berlin, pp 17–58

Hell R, Kruse C (2007) Sulfur in biotic interactions of plants. In: Hawkesford MJ, De Kok LJ (eds) Sulfur in plants—an ecological perspective. Springer, Berlin, pp 197–224

Hietz P, Turner BL, Wanek W, Richter A, Nock CA, Wright SJ (2011) Long-term change in the nitrogen cycle of tropical forests. Science 334:664–666

Hobbie EA, Ouimette AP (2009) Controls of nitrogen isotope patterns in soil profiles. Biogeochemistry 95:355–371

Holdaway RJ, Richardson SJ, Dickie IA, Peltzer DA, Coomes DA (2011) Species- and community-level patterns in fine root traits along a 120 000-year soil chronosequence in temperate rain forest. J Ecol 99:954–963

Jangid K, Whitman WB, Condron LM, Turner BL, Williams MA (2013) Soil bacterial community succession during long-term ecosystem development. Mol Ecol 22:3415–3424

Jehne W, Thompson CH (1981) Endomycorrhizae in plant colonization on sand-dunes at Cooloola, Australia. Aust J Ecol 6:221–230

Johnson DW (1984) Sulfur cycling in forests. Biogeochemistry 1:29–43

Kelly J, Lambert MJ (1972) The relationship between sulphur and nitrogen in the foliage of *Pinus radiata*. Plant Soil 37:395–407

Kirkby CA, Kirkegaard JA, Richardson AE, Wade LJ, Blanchard C, Batten G (2011) Stable soil organic matter: A comparison of C:N:P:S ratios in Australian and other world soils. Geoderma 163:197–208

Krouse HR, Coplen TB (1997) Reporting of relative sulfur isotope-ratio data. Pure Appl Chem 69:293–295

Krouse HR, Stewart JWB, Grinenko VA (1991) Pedosphere and biosphere. In: Krouse HR, Grinenko VA (eds) Stable isotopes in the assessment of natural and anthropogenic sulphur in the environment. Wiley, Chichester, pp 267–306

Kusakabe MTA, Rafter TA, Stout JD, Collie TW (1976) Sulphur isotopic variations in nature. 12. Isotopic ratios of sulphur extracted from some plants, soils and related materials. N Z J Sci 19:433–440

Laliberté E, Turner BL, Costes T, Pearse SJ, Wyrwoll K-H, Zemunik G, Lambers H (2012) Experimental assessment of nutrient limitation along a 2-million-year dune chronosequence in the south-western Australia biodiversity hotspot. J Ecol 100:631–642

Laliberté E, Zemunik G, Turner BL (2014) Environmental filtering explains variation in plant diversity along resource gradients. Science 345:1602–1605

Lambert MJ, Turner J (1998) Sulfur nutrition and cycling in Southern Hemisphere temperate and subtropical forest

ecosystems. In: Maynard DG (ed) Sulfur in the environment. Marcel Dekker Inc, New York, pp 263–293

Ledgard SF, Upsdell MP (1991) Sulphur inputs from rainfall throughout New Zealand. N Z J Agric Res 34:105–111

Lee WG (1988) Mineral element concentrations in foliage and bark of woody species on Auckland Island, New Zealand. N Z J Ecol 11:109–111

Lee WG, Johnson PN (1984) Mineral element concentrations in foliage of divaricate and non-divaricate *Coprosma* species. N Z J Ecol 7:169–174

Lehmann J, Solomon D, Zhao F-J, McGrath SP (2008) Atmospheric SO_2 emissions since the late 1800 s change organic sulfur forms in humic substance extracts of soils. Environ Sci Technol 42:3550–3555

Marschner H (2006) Mineral nutrition of higher plants. Academic Press, San Diego

Mathot M, Mertens J, Verlinden G, Lambert R (2008) Positive effects of sulphur fertilisation on grasslands yields and quality in Belgium. Eur J Agron 28:655–658

Mayer B, Feger KH, Giesemann A, Jäger H-J (1995) Interpretation of sulfur cycling in two catchments in the Black Forest (Germany) using stable sulfur isotopes and oxygen isotope data. Biogeochemistry 30:31–58

Maynard DG, Stewart JWB, Bettany JR (1984) Sulfur cycling in grassland and parkland soils. Biogeochemistry 1:97–111

McGill WB, Cole CV (1981) Comparative aspects of cycling of organic C, N, S, and P through soil organic matter. Geoderma 26:267–286

McGrath SP, Zhao FJ (1995) A risk assessment of sulphur deficiency in cereals using soil and atmospheric deposition data. Soil Use Manag 11:110–114

Mitchell MJ, David MB, Harrison RB (1992) Sulphur dynamics of forest ecosystems. In: Howarth RW, Stewart JWB, Ivanov MV (eds) SCOPE 48: sulfur cycling on the continents. Wiley, New York, pp 215–254

Morra MJ, Fendorf SE, Brown PD (1997) Speciation of S in humic and fulvic acids using X-ray absorbtion near-edge structure (XANES) spectroscopy. Geochim Cosmochim Acta 61:683–688

Parfitt RL, Smart RSC (1978) The mechanism of sulfate adsorption on iron oxides. Soil Sci Soc Am J 42:48–50

Parfitt RL, Ross DJ, Coomes DA, Richardson SJ, Smale MC, Dahlgren RA (2005) N and P in New Zealand soil chronosequences and relationships with foliar N and P. Biogeochemistry 75:305–328

Parton WJ, Stewart JWB, Cole CV (1988) Dynamics of C, N, P and S in grassland soils: a model. Biogeochemistry 5:109–131

Peltzer DA, Wardle DA, Allison VJ, Baisden WT, Bardgett RD, Chadwick OA, Condron LM, Parfitt RL, Porder S, Richardson SJ, Turner BL, Vitousek PM, Walker J, Walker LR (2010) Understanding ecosystem retrogression. Ecol Monogr 80:509–529

Prietzel J, Thieme J, Salome M, Knicker H (2007) Sulfur K-edge XANES spectroscopy reveals differences in sulfur speciation of bulk soils, humic acid, fulvic acid, and particle size seperates. Soil Biol Biochem 39:877–890

Prietzel J, Wu Y, Dümig A, Zhou J, Klysubun W (2013) Soil sulphur speciation in two glacier forefield soil chronosequences assessed by S *K*-edge XANES spectroscopy. Eur J Soil Sci 64:260–272

Reimann C, Koller F, Frengstad B, Kashulina G, Niskavaara H, Englmaier P (2003) Total sulphur in leaves of several plant species from nine catchments within a 1,500,000 km2 area in northern Europe: local vs. regional variability. Geochem 3:205–215

Richardson SJ, Peltzer DA, Allen RB, McGlone MS, Parfitt RL (2004) Rapid development of phosphorus limitation in temperate rainforest along the Franz Josef soil chronosequence. Oecologia 139:267–276

Richardson SJ, Peltzer DA, Allen RB, McGlone MS (2005) Resorption proficiency along a chronosequence: responses among communities and within species. Ecology 86:20–25

Schmalenberger A, Noll M (2010) Shifts in desulfonating bacterial communities along a soil chronosequence in the forefield of a receding glacier. FEMS Microbiol Ecol 71:208–217

Schroth AW, Bostick BC, Graham M, Kaste JM, Mitchell MJ, Friedland AJ (2007) Sulfur species behavior in soil organic matter during decomposition. J Geophys Res 112:G04011

Sinsabaugh RL, Hill BH, Shah JJF (2009) Ecoenzymatic stoichiometry of microbial organic nutrient acquisition in soil and sediment. Nature 462:795–799

Smith GS, Cornforth IS, Henderson HV (1985) Critical leaf concentrations for deficiencies of nitrogen, potassium, phosphorus, sulphur, and magnesium in perennial ryegrass. New Phytol 101:393–409

Solomon D, Lehmann J, Martínez CE (2003) Sulfur K-edge XANES spectroscopy as a tool for understanding sulfur dynamics in soil organic matter. Soil Sci Soc Am J 67:1721–1731

Solomon D, Lehmann J, Kinyangi J, Pell A, Theis J, Riha S, Ngoze S, Amelung W, Preez C, Machado S, Ellert B, Janzen H (2009) Anthropogenic and climate influences on biogeochemical dynamics and molecular-level speciation of soil sulfur. Ecol Appl 19:989–1002

Stevens PR (1968) A chronosequence of soils near the Franz Josef glacier. PhD thesis, Lincoln College. University of Canterbury, Canterbury, New Zealand, p 389

Stevenson FJ, Cole MA (1999) Cycles of soil: carbon, nitrogen, phosphorus, sulfur, micronutrients. Wiley, Chichester

Sutherland MD (1947) The odour of *Coprosma foetidissima*. N Z J Sci Technol 29:94–99

Syers JK, Adams JA, Walker TW (1970) Accumulation of organic matter in a chronosequence of soils developed on wind-blown sand in New Zealand. J Soil Sci 21:146–153

Tabatabai MA (1996) Sulfur. In: Sparks DL (ed) Methods of soil analysis, part 3—chemical methods. Soil Science Society of America and the American Society of Agronomy, Madison, pp 921–960

Tanikawa T, Hashimoto Y, Yamaguchi N, Ito Y, Fukushima S, Kanda K, Uemura M, Hasegawa T, Takahashi M, Yoshinaga S (2014) Sulfur accumulation in Melanudands during development by upbuilding pedogenesis since 14–15 cal. ka. Geoderma 232–234:609–618

Turner BL, Condron LM (2013) Pedogenesis, nutrient dynamics, and ecosystem development: the legacy of T.W. Walker and J.K. Syers. Plant Soil 367:1–10

Turner BL, Condron LM, Richardson SJ, Peltzer DA, Allison VJ (2007) Soil organic phosphorus transformations during pedogenesis. Ecosystems 10:1166–1181

Turner BL, Lambers H, Condron LM, Cramer MD, Leake JR, Richardson AE, Smith SE (2013) Soil microbial biomass and the fate of phosphorus during long-term ecosystem development. Plant Soil 367:225–234

Vet R, Artz RS, Carou S, Shaw M, Ro C-U, Aas W, Baker A, Bowersox VC, Dentener F, Galy-Lacaux C, Hou A, Pienaar JJ, Gillett R, Forti MC, Gromov S, Hara H, Khodzher T, Mahowald NM, Nickovic S, Rao PSP, Reid NW (2014) A global assessment of precipitation chemistry and deposition of sulfur, nitrogen, sea salt, base cations, organic acids, acidity and pH, and phosphorus. Atmos Environ 93:3–100

Vitousek PM (2004) Nutrient cycling and limitation. Princeton University Press, Princeton

Vitousek PM, Farrington H (1997) Nutrient limitation and soil development: experimental test of a biogeochemical theory. Biogeochemistry 37:63–75

Vitousek PM, Matson P, Van Cleve K (1989) Nitrogen availability and nitrification during succession: primary, secondary, and old-field seres. Plant Soil 115:229–239

Walker TW, Adams AFR (1958) Studies on soil organic matter: I. influence of phosphorus content of parent materials on accumulations of carbon, nitrogen, sulfur, and organic phosphorus in grassland soils. Soil Sci 85:307–318

Walker TW, Adams AFR (1959) Studies on soil organic matter: 2: Influence of increased leaching at various stages of weathering on levels of carbon, nitrogen, sulfur, and organic and total phosphorus. Soil Sci 87:1–10

Walker TW, Syers JK (1976) The fate of phosphorus during pedogenesis. Geoderma 15:1–19

Wardle P (1980) Primary succession in Westland National Park and its vicinity, New Zealand. N Z J Bot 18:221–232

Wardle DA, Walker LR, Bardgett RD (2004) Ecosystem properties and forest decline in contrasting long-term chronosequences. Science 305:509–513

Williamson WM, Wardle DA, Yeates GW (2005) Changes in soil microbial and nematode communities during ecosystem decline across a long-term chronosequence. Soil Biol Biochem 37:1289–1301

Wright SJ, Yavitt JB, Wurzburger N, Turner BL, Tanner EVJ, Sayer EJ, Santiago LS, Kaspari M, Hedin LO, Harms KE, Garcia MN, Corre MD (2011) Potassium, phosphorus or nitrogen limit root allocation, tree growth and litter production in a lowland tropical forest. Ecology 92:1616–1625

Wu J, O'Donnell AG, He ZL, Syers JK (1994) Fumigation-extraction method for the measurement of soil microbial biomass-S. Soil Biol Biochem 26:117–125

Xia K, Weesner F, Bleam WF, Bloom PR, Skyllberg UL, Helmke PA (1998) XANES studies of oxidation states in aquatic and soil humic substances. Soil Sci Soc Am J 62:1240–1246

Zhao FJ, Wu J, McGrath SP (1996) Soil organic sulphur and its turnover. In: Piccolo A (ed) Humic substances in terrestrial ecosystems. Elsevier Science, Amsterdam, pp 467–506

Zhao FJ, Lehmann J, Solomon D, Fox MA, McGrath SP (2006) Sulphur speciation and turnover in soils: evidence from sulphur K-edge XANES spectroscopy and isotope dilution studies. Soil Biol Biochem 38:1000–1007